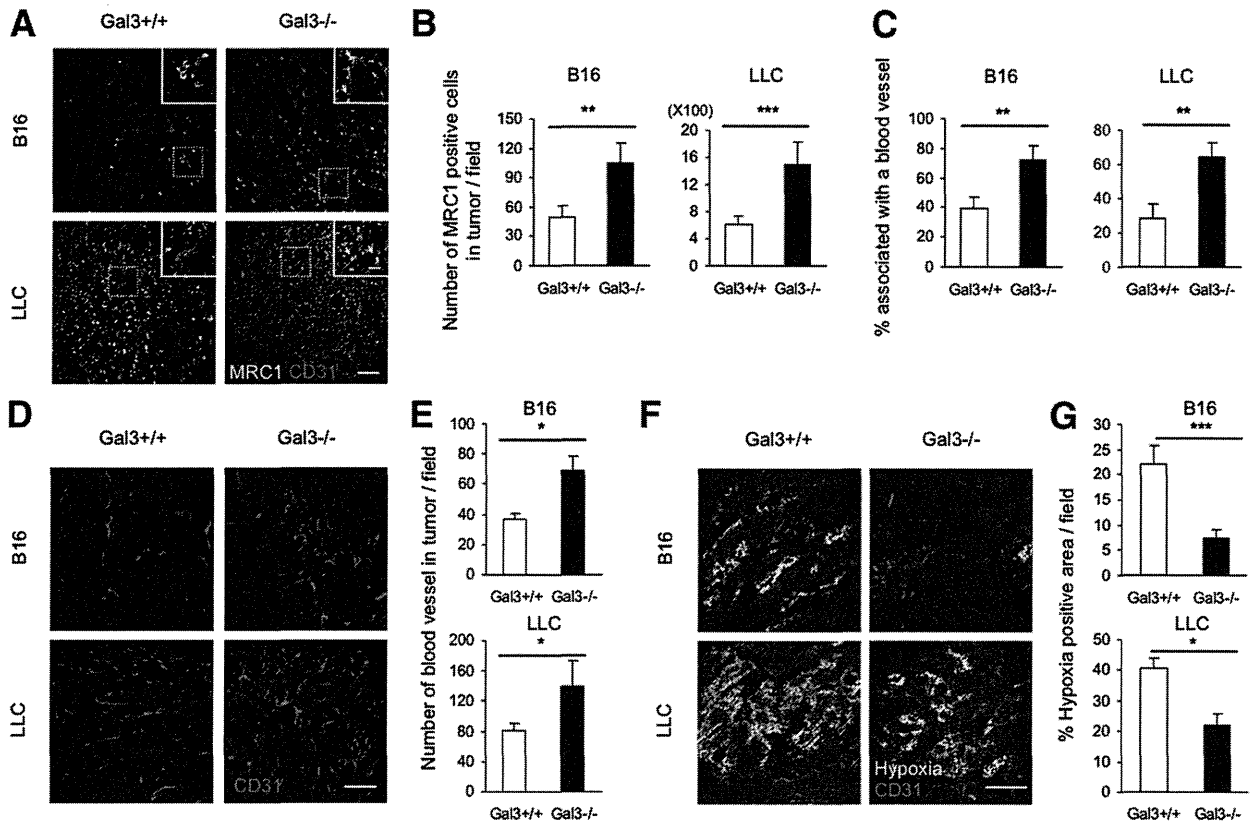

Figure 4 Increased tumor angiogenesis with M2 macrophage infiltration in *Gal3*$^{-/-}$ mice. **A:** Immunofluorescence staining of MRC1 (green) and CD31 (red) in the B16 or LLC tumor sections from *Gal3*$^{+/+}$ or *Gal3*$^{-/-}$ mice. **Dashed boxes** indicate areas shown at higher magnification. **Arrows** indicate focal MRC1-positive cells closely localizing to blood vessels. Scale bar = 100 μm and 25 μm (**inset**). **B:** Quantitative evaluation of the number of MRC1-positive macrophages in B16 tumor (**left**) or LLC tumor (**right**) sections from *Gal3*$^{+/+}$ or *Gal3*$^{-/-}$ mice. Data are means ± SEM. $^{**}P < 0.01$, $^{***}P < 0.001$ (five random fields of four independent tumor sections). **C:** Percentage of MRC1-positive macrophages closely localizing to blood vessels in B16 tumor (**left**) or LLC tumor (**right**) sections from *Gal3*$^{+/+}$ or *Gal3*$^{-/-}$ mice. Data are means ± SEM. $^{**}P < 0.01$ (five random fields of four independent tumor sections). **D:** Immunofluorescence staining of CD31 (red) in the B16 or LLC tumor sections derived from *Gal3*$^{+/+}$ or *Gal3*$^{-/-}$ mice. Scale bar = 200 μm. **E:** Quantification of the number of blood vessels as in **D**. Data are means ± SEM. $^{*}P < 0.05$ (five random fields of four independent tumor sections). **F:** Immunofluorescence staining of CD31 (red) in the B16 or LLC tumor sections from *Gal3*$^{+/+}$ or *Gal3*$^{-/-}$ mice. Hypoxic status was revealed by HypoxyProbe (green). Scale bar = 500 μm. **G:** Quantification of the hypoxic area in B16 or LLC tumor sections from *Gal3*$^{+/+}$ or *Gal3*$^{-/-}$ mice. Data are means ± SEM. $^{*}P < 0.05$, $^{***}P < 0.001$ (five random fields of 10 independent tumor sections).

mice] (Figure 5A). We generated control mice in which bone marrow of *Gal3*$^{+/+}$ animals was replaced with that of *Gal3*$^{+/+}$ mice [*Gal3*$^{+/+}$ (BM-T) mice].

After BM-T, we confirmed that bone marrow cells did express Gal-3 in the *Gal3*$^{-/-}$ (BM-T) mice (Figure 5B). Enhancement of both B16 and LLC tumor growth was abrogated completely in *Gal3*$^{-/-}$ (BM-T) mice (Figure 5, C–H). In terms of macrophage infiltration, the number of F4/80-positive cells in the tumor microenvironment was not significantly different between *Gal3*$^{-/-}$ (BM-T) mice and *Gal3*$^{+/+}$ (BM-T) mice (Figure 6, A and B). This was also the case when the number of MRC1-positive cells and the number of these cells closely associating with CD31-positive blood vessels in the tumor microenvironment was quantified (Figure 6, C–E). Attenuation of enhancement of macrophage infiltration into tumors developing in *Gal3*$^{-/-}$ (BM-T) mice also was accompanied by restoration of angiogenesis to a level observed in *Gal3*$^{+/+}$ (BM-T) host tumors (Figure 6, C–E). Therefore, we conclude that lack of Gal-3 in bone marrow cells is responsible for the enhanced migration of macrophages into the tumor microenvironment, and that this facilitates tumor growth.

Discussion

We analyzed the functional role of tumor environmental Gal-3 in tumor growth. Although several functions of Gal-3 in a variety of cells, such as immune cells, neuronal cells, epithelial cells, cancer cells, and others, have been suggested,[12,28] we focused on macrophages. It has been reported that recombinant Gal-3 induces chemotaxis of monocytes/macrophages; however, the *in vivo* relevance of this for tumor growth had not been analyzed. We report that Gal-3 produced by the tumor induces macrophage migration, resulting in the promotion of angiogenesis and tumor growth.

There are two modes of action of Gal-3 (ie, mediated by intracellular Gal-3), especially in the nucleus, or secreted

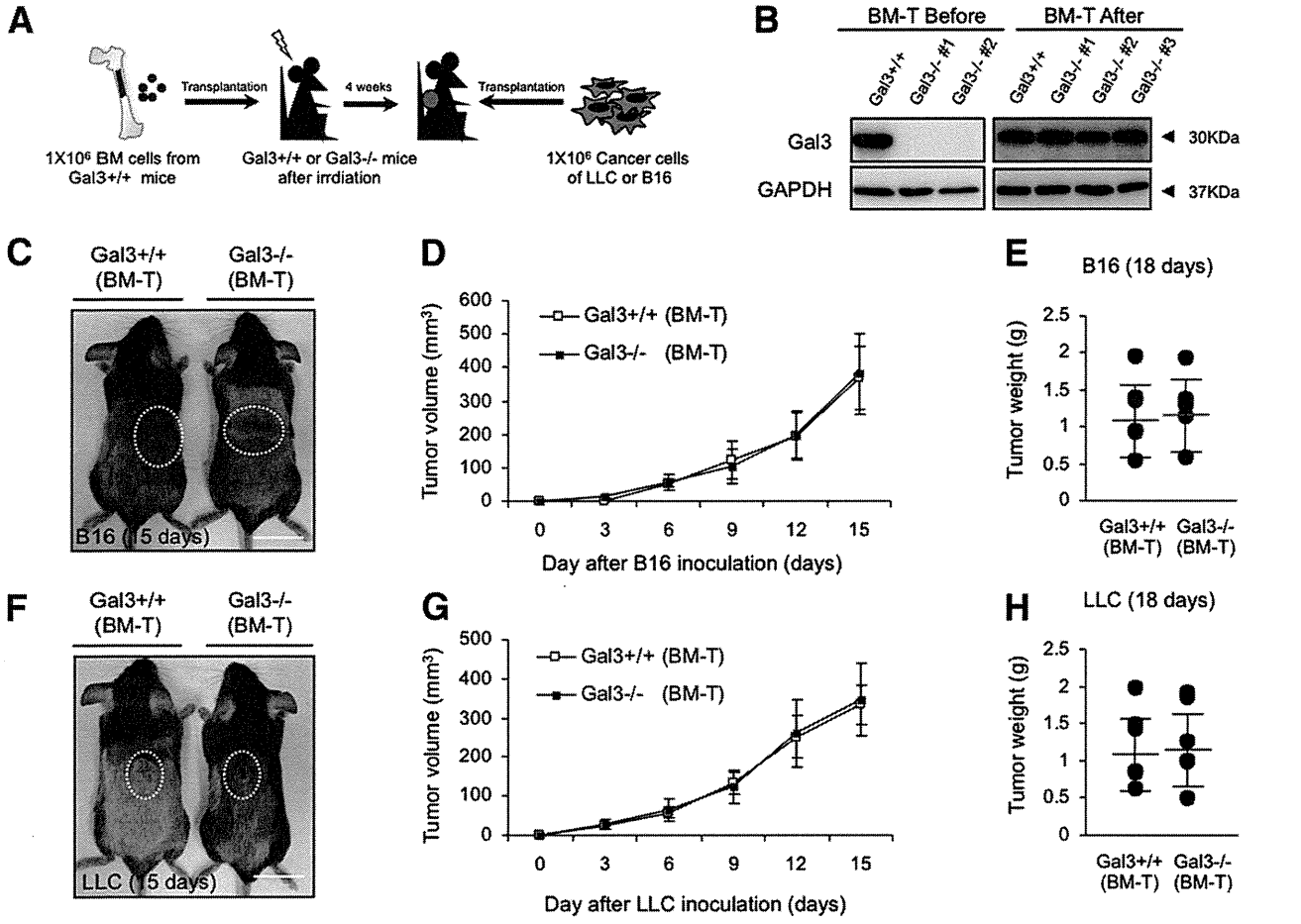

Figure 5 Tumor growth in *Gal3*$^{-/-}$ mice transplanted with wild-type bone marrow cells. **A:** The experimental scheme of BM-T and the tumor cell allograft model. For details, see *Materials and Methods*. **B:** Western blot analysis of Gal-3 expression in bone marrow cells 4 weeks after BM-T in *Gal3*$^{-/-}$ mice as in **A**. Numbers 1, 2, and 3 are different individual mice. Bone marrow cells from *Gal3*$^{+/+}$ mice were used as the positive control. **C:** Gross appearance of B16 tumors developing in BM-T—treated *Gal3*$^{+/+}$ and *Gal3*$^{-/-}$ mice on day 15 after tumor cell inoculation. **Dashed lines** indicate tumor area. Scale bars: 2 cm. **D:** Tumor growth curves of B16 cells on s.c. injection into *Gal3*$^{+/+}$ (BM-T) or *Gal3*$^{-/-}$ (BM-T) mice as in **C** (n = 10). **E:** Tumor weight 18 days after B16 cell inoculation as in **C** (n = 7). **F:** Gross appearance of LLC tumors developing in BM-T—treated *Gal3*$^{+/+}$ and *Gal3*$^{-/-}$ mice on day 15 after tumor cell inoculation. **Dashed lines** indicate tumor area. Scale bars: 2 cm. **G:** Tumor growth curves of LLC cells on s.c. injection into *Gal3*$^{+/+}$ (BM-T) or *Gal3*$^{-/-}$ (BM-T) mice as in **F** (n = 10). **H:** Tumor weight 18 days after LLC cell inoculation as in **F** (n = 7). Data are means ± SEM. GAPDH, glyceraldehyde-3-phosphate dehydrogenase.

Gal-3. In the case of intracellular action, Gal-3 as a component of the heterogeneous nuclear ribonuclear protein is a factor in pre-mRNA splicing to control cell cycling and prevent apoptosis possibly mediated through interaction with Bcl-2 family members.[29,30] On the other hand, the secreted form of Gal-3 regulates cell adhesion and migration through cell-cell and cell-extracellular matrix interactions.[31,32] In terms of myeloid cell lineages, it has been reported that exogenous Gal-3 affects apoptosis of neutrophils in a context-dependent manner[33] and induces mediator release from both IgE-sensitized and IgE-nonsensitized mast cells.[34,35] Here, we analyzed Gal-3 secreted from tumors for its action on macrophages. It has been reported that Gal-3 production is observed in immune cells, epithelial cells, and neuronal cells.[12,31] To analyze the migration of macrophages into the tumor microenvironment more precisely, attenuation of Gal-3 expression by all cells except tumor cells is required. In our system, we used *Gal3*$^{-/-}$ mice as an allograft host and two Gal-3-producing cancer cell lines that established tumors generating a concentration gradient of Gal-3, enabling us to visualize macrophage migration.

Macrophages in the tumor microenvironment are termed tumor-associated macrophages and their number correlates with the malignancy of the tumor.[36] It is widely accepted that tumor-associated macrophages promote angiogenesis, which stimulates tumor growth.[25,26] In our present work, we found that the Gal-3 concentration gradient effectively induced migration of M2-like macrophages. It is well known that there are two types of macrophages. One is termed M1, which are macrophages differentiated and activated by lipopolysaccharide and the proinflammatory cytokine interferon-γ. M1 macrophages produce high levels of oxidative metabolites and proinflammatory cytokines for host defense and tumor cell death.[37,38] On the other hand, M2 macrophages activated by IL4 or IL13 promote angiogenesis and also matrix remodeling.[39–41] Therefore, a high frequency of M2 macrophages as observed in tumors developing in *Gal3*$^{-/-}$ mice correlates with robust angiogenesis in this model.

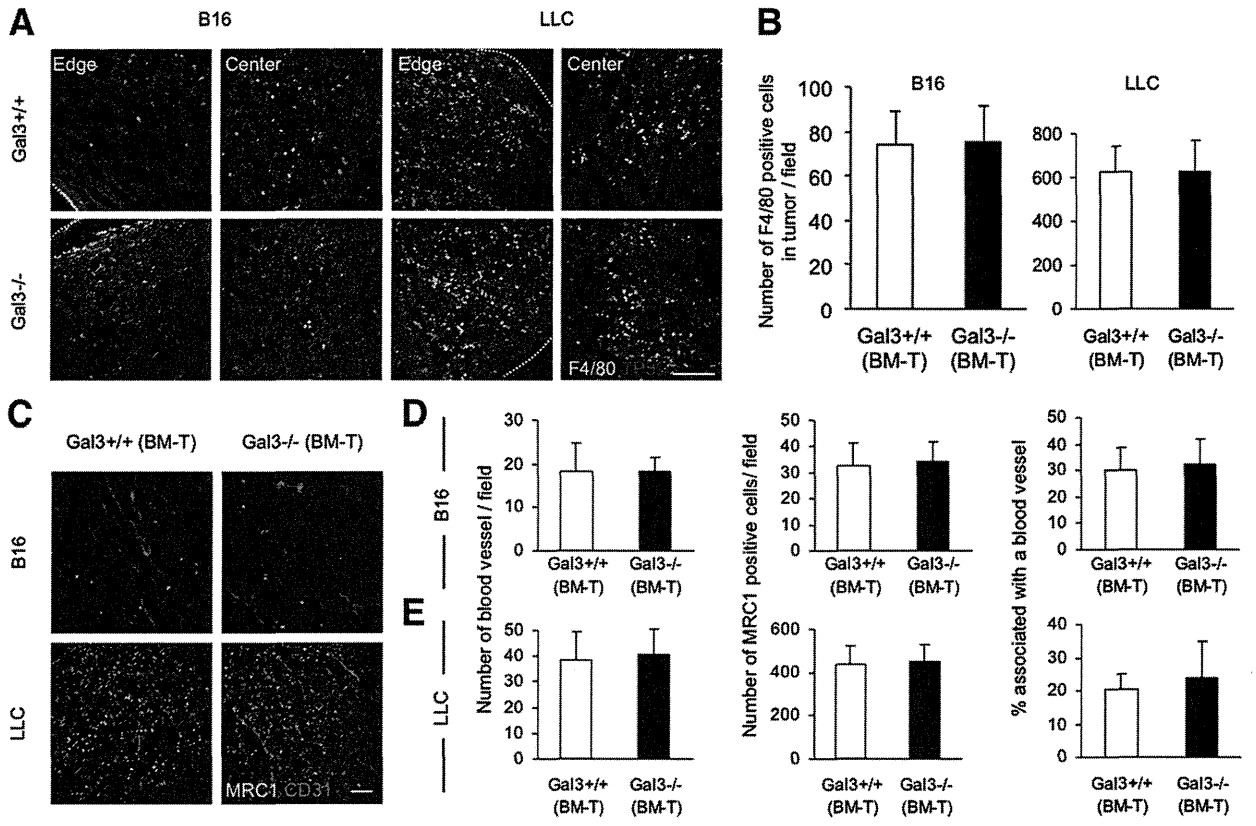

Figure 6 Infiltration of macrophages and tumor angiogenesis in *Gal3*$^{-/-}$ mice transplanted with WT bone marrow cells. **A:** Immunofluorescence staining of F4/80 (green) and TO-PRO-3 (blue) in the B16 or LLC tumor sections from *Gal3*$^{+/+}$ (BM-T) or *Gal3*$^{-/-}$ (BM-T) mice as in Figure 5C. Scale bars: 200 μm. **B:** Quantification of the number of F4/80-positive macrophages in B16 or LLC tumor sections from *Gal3*$^{+/+}$ (BM-T) or *Gal3*$^{-/-}$ (BM-T) mice. Data are means ± SEM (five random fields of seven independent tumor sections). **C:** Immunofluorescence staining of MRC1 (green) and CD31 (red) in the B16 or LLC tumor sections from *Gal3*$^{+/+}$ (BM-T) or *Gal3*$^{-/-}$ (BM-T) mice. Scale bars: 100 μm. **D** and **E:** Quantification of the number of blood vessels (**left**), of MRC1-positive macrophages (**middle**), and of MRC1-positive cells closely associating with blood vessels (**right**) in B16 (**D**) or LLC (**E**) tumor sections from *Gal3*$^{+/+}$ (BM-T) or *Gal3*$^{-/-}$ (BM-T) mice. Data are means ± SEM (five random fields of seven independent tumor sections).

Interestingly, we found that MRC1-positive M2-like macrophages express lower levels of Gal-3 than MRC-negative macrophages. When cells abundantly express Gal-3, they may not use remotely produced Gal-3 for their chemoattractive migration toward the Gal-3-producing area. Therefore, Gal-3 expression needs to be attenuated for testing cell migration toward Gal-3. In our analysis, J774 macrophages in which Gal-3 had been knocked down, or macrophages from *Gal3*$^{-/-}$ mice, more effectively migrate toward Gal-3 than the parental J774 cells or macrophages derived from *Gal3*$^{+/+}$ mice, respectively. These results suggest that M2 macrophages have the ability to migrate along Gal-3 concentration gradients.

In our present model, we injected LLC lung cancer cells subcutaneously, so this was a nonorthotopic model. Because melanoma occurs in the skin, subcutaneous B16 injection may be viewed as an orthotopic model. In tumor progression, interactions between host cells and tumor cells influence both angiogenesis and metastasis.[42] Therefore, in addition to the nonorthotopic model using LLC cells, we inoculated these cells into the lung and observed the effects of Gal-3. The results suggest that Gal-3 from tumor cells induces migration of M2 macrophages and angiogenesis in an orthotopic model (Supplemental Figure S1[43]). This further suggests that Gal-3 from metastatic as well as primary tumor induces macrophage migration into the tumor.

Our present model using *Gal3*$^{-/-}$ mice as a tumor host recapitulates the tumor condition in which expression of Gal-3 in the tumor increases. It has been reported that Gal-3 directly induces endothelial tube formation.[19,44] Therefore, higher levels of Gal-3 induce angiogenesis directly affecting ECs within the tumor; however, macrophage recruitment by Gal-3 also may be involved in the acceleration of tumor angiogenesis. In summary, knowledge of Gal-3 expression may help in the assessment of cancer patient status. Indeed, one line of evidence suggests that Gal-3 expression levels are related to the degree of biological aggressiveness in human colorectal tumors.[45] Therefore, suppression of the function or expression of Gal-3 may be a promising approach for cancer therapy.

Acknowledgments

We thank Dr. Daniel K. Hsu, Dr. Fu-Tong Liu (University of California), and Dr. Koichi Hiraga (University of

Toyama, Japan) for providing *Gal3*$^{-/-}$ mice; Noriko Fujimoto for preparation of plasmid DNA; and Keisho Fukuhara for administrative assistance.

Supplemental Data

Supplemental material for this article can be found at *http://dx.doi.org/10.1016/j.ajpath.2013.01.017.*

References

1. Carmeliet P: Angiogenesis in health and disease. Nat Med 2003, 9: 653–660
2. Carmeliet P: Angiogenesis in life, disease and medicine. Nature 2005, 438:932–936
3. Coussens LM, Werb Z: Inflammation and cancer. Nature 2002, 420: 860–867
4. Takakura N, Watanabe T, Suenobu S, Yamada Y, Noda T, Ito Y, Satake M, Suda T: A role for hematopoietic stem cells in promoting angiogenesis. Cell 2000, 102:199–209
5. Yamada Y, Takakura N: Physiological pathway of differentiation of hematopoietic stem cell population into mural cells. J Exp Med 2006, 203:1055–1065
6. Kessenbrock K, Plaks V, Werb Z: Matrix metalloproteinases: regulators of the tumor microenvironment. Cell 2010, 141:52–67
7. Coffelt SB, Tal AO, Scholz A, De Palma M, Patel S, Urbich C, Biswas SK, Murdoch C, Plate KH, Reiss Y, Lewis CE: Angiopoietin-2 regulates gene expression in TIE2-expressing monocytes and augments their inherent proangiogenic functions. Cancer Res 2010, 70: 5270–5280
8. Mazzieri R, Pucci F, Moi D, Zonari E, Ranghetti A, Berti A, Politi LS, Gentner B, Brown JL, Naldini L, De Palma M: Targeting the ANG2/TIE2 axis inhibits tumor growth and metastasis by impairing angiogenesis and disabling rebounds of proangiogenic myeloid cells. Cancer Cell 2011, 19:512–526
9. Qian BZ, Pollard JW: Macrophage diversity enhances tumor progression and metastasis. Cell 2010, 141:39–51
10. Grivennikov SI, Greten FR, Karin M: Immunity, inflammation, and cancer. Cell 2010, 140:883–899
11. Barondes SH, Castronovo V, Cooper DN, Cummings RD, Drickamer K, Feizi T, Gitt MA, Hirabayashi J, Hughes C, Kasai K, Leffler H, Liu F, Lotan R, Mercurio AM, Monsigny M, Pillai S, Poirer F, Raz A, Rigby PW, Rini JM, Wang JL: Galectins: a family of animal beta-galactoside-binding lectins. Cell 1994, 76:597–598
12. Dumic J, Dabelic S, Flögel M: Galectin-3: an open-ended story. Biochim Biophys Acta 2006, 1760:616–635
13. Sano H, Hsu DK, Yu L, Apgar JR, Kuwabara I, Yamanaka T, Hirashima M, Liu FT: Human galectin-3 is a novel chemoattractant for monocytes and macrophages. J Immunol 2000, 165:2156–2164
14. Radosavljevic G, Volarevic V, Jovanovic I, Milovanovic M, Pejnovic N, Arsenijevic N, Hsu DK, Lukic ML: The roles of Galectin-3 in autoimmunity and tumor progression. Immunol Res 2012, 52: 100–110
15. Hsu DK, Yang RY, Pan Z, Yu L, Salomon DR, Fung-Leung WP, Liu FT: Targeted disruption of the galectin-3 gene results in attenuated peritoneal inflammatory responses. Am J Pathol 2000, 156: 1073–1083
16. Naito H, Kidoya H, Sakimoto S, Wakabayashi T, Takakura N: Identification and characterization of a resident vascular stem/progenitor cell population in preexisting blood vessels. EMBO J 2011, 31: 842–855
17. Kidoya H, Naito H, Takakura N: Apelin induces enlarged and nonleaky blood vessels for functional recovery from ischemia. Blood 2010, 115:3166–3174
18. Huang X, Yamada Y, Kidoya H, Naito H, Nagahama Y, Kong L, Katoh SY, Li WL, Ueno M, Takakura N: EphB4 overexpression in B16 melanoma cells affects arterial-venous patterning in tumor angiogenesis. Cancer Res 2007, 67:9800–9808
19. Nangia-Makker P, Honjo Y, Sarvis R, Akahani S, Hogan V, Pienta KJ, Raz A: Galectin-3 induces endothelial cell morphogenesis and angiogenesis. Am J Pathol 2000, 156:899–909
20. Hsu DK, Chernyavsky AI, Chen HY, Yu L, Grando SA, Liu FT: Endogenous galectin-3 is localized in membrane lipid rafts and regulates migration of dendritic cells. J Invest Dermatol 2009, 129: 573–583
21. Leek RD, Harris AL: Tumor-associated macrophages in breast cancer. J Mammary Gland Biol Neoplasia 2002, 7:177–189
22. Lin EY, Li JF, Bricard G, Wang W, Deng Y, Sellers R, Porcelli SA, Pollard JW: Vascular endothelial growth factor restores delayed tumor progression in tumors depleted of macrophages. Mol Oncol 2007, 1: 288–302
23. Giraudo E, Inoue M, Hanahan D: An amino-bisphosphonate targets MMP-9-expressing macrophages and angiogenesis to impair cervical carcinogenesis. J Clin Invest 2004, 114:623–633
24. Satoh T, Takeuchi O, Vandenbon A, Yasuda K, Tanaka Y, Kumagai Y, Miyake T, Matsushita K, Okazaki T, Saitoh T, Honma K, Matsuyama T, Yui K, Tsujimura T, Standley DM, Nakanishi K, Nakai K, Akira S: The Jmjd3-Irf4 axis regulates M2 macrophage polarization and host responses against helminth infection. Nat Immunol 2010, 11:936–944
25. Sica A, Allavena P, Mantovani A: Cancer related inflammation: the macrophage connection. Cancer Lett 2008, 267:204–215
26. Solinas G, Germano G, Mantovani A, Allavena P: Tumor-associated macrophages (TAM) as major players of the cancer-related inflammation. J Leukoc Biol 2009, 86:1065–1073
27. Noguera-Troise I, Daly C, Papadopoulos NJ, Coetzee S, Boland P, Gale NW, Lin HC, Yancopoulos GD, Thurston G: Blockade of Dll4 inhibits tumour growth by promoting non-productive angiogenesis. Nature 2006, 444:1032–1037
28. Nangia-Makker P, Balan V, Raz A: Regulation of tumor progression by extracellular galectin-3. Cancer Microenviron 2008, 1:43–51
29. Dagher SF, Wang JL, Patterson RJ: Identification of galectin-3 as a factor in pre-mRNA splicing. Proc Natl Acad Sci U S A 1995, 92: 1213–1217
30. Haudek KC, Spronk KJ, Voss PG, Patterson RJ, Wang JL, Arnoys EJ: Dynamics of galectin-3 in the nucleus and cytoplasm. Biochim Biophys Acta 2010, 1800:181–189
31. Califice S, Castronovo V, Van Den Brûle F: Galectin-3 and cancer (review). Int J Oncol 2004, 25:983–992
32. Perillo NL, Marcus ME, Baum LG: Galectins: versatile modulators of cell adhesion, cell proliferation, and cell death. J Mol Med 1998, 76: 402–412
33. Karlsson A, Christenson K, Matlak M, Björstad A, Brown KL, Telemo E, Salomonsson E, Leffler H, Bylund J: Galectin-3 functions as an opsonin and enhances the macrophage clearance of apoptotic neutrophils. Glycobiology 2009, 19:16–20
34. Frigeri LG, Liu FT: Surface expression of functional IgE binding protein, an endogenous lectin, on mast cells and macrophages. J Immunol 1992, 148:861–867
35. Liu FT, Frigeri LG, Gritzmacher CA, Hsu DK, Robertson MW, Zuberi RI: Expression and function of an IgE-binding animal lectin (epsilon BP) in mast cells. Immunopharmacology 1993, 26: 187–195
36. Allavena P, Mantovani A: Immunology in the clinic review series; focus on cancer: tumour-associated macrophages: undisputed stars of the inflammatory tumour microenvironment. Clin Exp Immunol 2012, 167:195–205
37. Mosser DM, Edwards JP: Exploring the full spectrum of macrophage activation. Nat Rev Immunol 2008, 8:958–969
38. Benoit M, Desnues B, Mege JL: Macrophage polarization in bacterial infections. J Immunol 2008, 181:3733–3739

39. Bronte V, Zanovello P: Regulation of immune responses by L-arginine metabolism. Nat Rev Immunol 2005, 5:641–654
40. Mantovani A, Sica A, Sozzani S, Allavena P, Vecchi A, Locati M: The chemokine system in diverse forms of macrophage activation and polarization. Trends Immunol 2004, 25:677–686
41. Stein M, Keshav S, Harris N, Gordon S: Interleukin 4 potently enhances murine macrophage mannose receptor activity: a marker of alternative immunologic macrophage activation. J Exp Med 1992, 176:287–292
42. Fidler IJ: Critical determinants of metastasis. Semin Cancer Biol 2002, 12:89–96
43. Takizawa H, Kondo K, Toba H, Kenzaki K, Sakiyama S, Tangoku A: Fluorescence diagnosis of lymph node metastasis of lung cancer in a mouse model. Oncol Rep 2009, 22:17–21
44. Markowska AI, Liu FT, Panjwani N: Galectin-3 is an important mediator of VEGF- and bFGF-mediated angiogenic response. J Exp Med 2010, 207:1981–1993
45. Legendre H, Decaestecker C, Nagy N, Hendlisz A, Schüring MP, Salmon I, Gabius HJ, Pector JC, Kiss R: Prognostic values of galectin-3 and the macrophage migration inhibitory factor (MIF) in human colorectal cancers. Mod Pathol 2003, 16:491–504

The American Journal of Pathology, Vol. 181, No. 3, September 2012

http://dx.doi.org/10.1016/j.ajpath.2012.05.023

Tumorigenesis and Neoplastic Progression

Dual Inhibition of Met Kinase and Angiogenesis to Overcome HGF-Induced EGFR-TKI Resistance in *EGFR* Mutant Lung Cancer

Shinji Takeuchi,* Wei Wang,*† Qi Li,*‡ Tadaaki Yamada,* Kenji Kita,* Ivan S. Donev,* Takahiro Nakamura,§ Kunio Matsumoto,§ Eiji Shimizu,¶ Yasuhiko Nishioka,‖ Saburo Sone,‖ Takayuki Nakagawa,*,** Toshimitsu Uenaka,** and Seiji Yano*

From the Divisions of Medical Oncology and Tumor Dynamics and Regulation,§ Cancer Research Institute, Kanazawa University, Kanazawa, Japan; the Departments of Radiation Oncology† and Gastroenterology,‡ Nanfang Hospital, Southern Medical University, Guangzhou, China; the Division of Medical Oncology and Molecular Respirology,¶ Faculty of Medicine, Tottori University, Yonago, Japan; the Department of Respiratory Medicine and Rheumatology,‖ University of Tokushima Graduate School, Tokushima, Japan; and the Tsukuba Research Laboratories,** Eisai Co. Ltd., Tsukuba, Japan*

Acquired resistance to epidermal growth factor receptor (EGFR) tyrosine kinase inhibitors (TKIs) is a serious problem in the management of *EGFR* mutant lung cancer. We recently reported that hepatocyte growth factor (HGF) induces resistance to EGFR-TKIs by activating the Met/PI3K pathway. HGF is also known to induce angiogenesis in cooperation with vascular endothelial growth factor (VEGF), which is an important therapeutic target in lung cancer. Therefore, we hypothesized that dual inhibition of HGF and VEGF may be therapeutically useful for controlling HGF-induced EGFR-TKI–resistant lung cancer. We found that a dual Met/VEGF receptor 2 kinase inhibitor, E7050, circumvented HGF-induced EGFR-TKI resistance in *EGFR* mutant lung cancer cell lines by inhibiting the Met/Gab1/PI3K/Akt pathway *in vitro*. HGF stimulated VEGF production by activation of the Met/Gab1 signaling pathway in *EGFR* mutant lung cancer cell lines, and E7050 showed an inhibitory effect. In a xenograft model, tumors produced by HGF-transfected Ma-1 (Ma-1/HGF) cells were more angiogenic than vector control tumors and showed resistance to gefitinib. E7050 alone inhibited angiogenesis and retarded growth of Ma-1/HGF tumors. E7050 combined with gefitinib induced marked regression of tumor growth. Moreover, dual inhibition of HGF and VEGF by neutralizing antibodies combined with gefitinib also markedly regressed tumor growth. These results indicate the therapeutic rationale of dual targeting of HGF-Met and VEGF–VEGF receptor 2 for overcoming HGF-induced EGFR-TKI resistance in *EGFR* mutant lung cancer. ***(Am J Pathol 2012, 181:1034–1043; http://dx.doi.org/10.1016/j.ajpath.2012.05.023)***

Lung cancer is the leading cause of malignancy-related death worldwide. Recently, two types of molecularly targeted therapy, epidermal growth factor receptor (EGFR) tyrosine kinase inhibitors (TKIs) and the angiogenesis inhibitor bevacizumab, have been successfully introduced in the treatment of lung cancer.[1] The reversible EGFR-TKIs gefitinib and erlotinib show dramatic therapeutic efficacy in patients with *EGFR*-activating mutations, such as in-frame deletion in exon 19 and L858 point mutation in exon 21.[2,3] Bevacizumab, an anti–vascular endothelial growth factor (VEGF) antibody (Ab), enhances the efficacy of cytotoxic chemotherapy and prolongs survival in nonsquamous non–small-cell lung cancer.[4] However, disease progression due to intrinsic or acquired resistance always occurs even in cases treated with these molecularly targeted drugs. In fact, although reversible EGFR-TKIs show a response rate of

Supported by Grants-in-Aid for Cancer Research (21390256 to S.Y.); Scientific Research on Innovative Areas "Integrative Research on Cancer Microenvironment Network" from the Ministry of Education, Culture, Sports, Science, and Technology of Japan (22112010A01 to S.Y.); and Eisai Co. Ltd. and National Natural Science Foundation of China (81172243 to W.W.).

Accepted for publication May 17, 2012.

S.Y. obtained research grants from Eisai Co. Ltd. and Chugai Pharm and speaker fees from Chugai Pharma and AstraZeneca. T. Nakag. and T.U. are employees of Eisai Co. Ltd.

Supplemental material for this article can be found at *http://ajp.amjpathol.org* or at *http://dx.doi.org/10.1016/j.ajpath.2012.05.023*.

Address reprint requests to Seiji Yano, M.D., Ph.D., Division of Medical Oncology, Cancer Research Institute, Kanazawa University, Kanazawa, Ishikawa 920-0934, Japan. E-mail: syano@staff.kanazawa-u.ac.jp.

70% to 80% and significantly longer progression-free survival compared with standard first-line cytotoxic chemotherapy in *EGFR* mutant lung cancer,[5,6] patients almost always develop acquired resistance to EGFR-TKIs after varying periods.[7] In addition, 20% to 30% of patients with *EGFR*-activating mutations exhibit intrinsic resistance to EGFR-TKIs.[7] Therefore, intrinsic and acquired resistance to EGFR-TKIs is a major problem in the management of *EGFR* mutant lung cancer.

Recent studies documented three clinically relevant mechanisms—*EGFR* T790M secondary mutation (T790M secondary mutation),[8,9] *Met* gene amplification,[10] and hepatocyte growth factor (HGF) overexpression[11]— that induce acquired resistance to EGFR-TKIs in *EGFR* mutant lung cancer. Of these mechanisms, HGF overexpression is involved in not only acquired resistance but also intrinsic resistance. Moreover, recent studies indicated at least three important roles of HGF in EGFR-TKI resistance in *EGFR* mutant lung cancer. First, HGF induces resistance to the reversible EGFR-TKIs gefitinib and erlotinib by restoring the Met/Gab1/PI3K/Akt pathways.[11–13] Second, HGF accelerates expansion of preexisting *Met*-amplified cancer cells and facilitates Met amplification–mediated resistance during EGFR-TKI treatment.[13] Third, after acquiring resistance to reversible EGFR-TKIs, HGF induces resistance of lung cancer cells with T790M secondary mutation to irreversible EGFR-TKIs.[14] Furthermore, HGF is frequently co-expressed with T790M second mutation in *EGFR*[13,15] and *MET* gene amplification[13] in tumors of patients with acquired resistance to EGFR-TKIs. Consistently, although some irreversible EGFR inhibitors are in clinical development for use in patients with lung cancer refractory to gefitinib or erlotinib, the early results are disappointing.[16,17] These findings strongly suggest that HGF is an important therapeutic target for overcoming resistance to EGFR-TKIs.

VEGF activates VEGF receptor 2 (VEGFR-2) and plays crucial roles in angiogenesis in non–small-cell lung cancer.[18] HGF is also known to induce angiogenesis in cooperation with VEGF,[19,20] which is thought to be an important therapeutic target in lung cancer.[1,18] Therefore, we hypothesized that dual inhibition of HGF-Met and VEGF–VEGFR-2 may be therapeutically useful for controlling HGF-induced EGFR-TKI–resistant lung cancer. E7050 is an orally active dual TKI for Met and VEGFR-2.[21] It inhibits proliferation of several *Met* gene–amplified cancer cells and tumor angiogenesis, resulting in marked tumor regression and prolongation of the lifespan of tumor-bearing mice.[21] Based on these promising preclinical results, E7050 is currently under evaluation in clinical trials. In the present study, we determined the effect of dual inhibition of HGF-Met and VEGF–VEGFR-2 on HGF-induced EGFR-TKI resistance of *EGFR* mutant lung cancer cells using E7050 as well as anti-HGF Ab and anti-VEGF Ab.

Materials and Methods

Cell Culture

The *EGFR* mutant human lung adenocarcinoma cell lines PC-9[11] and Ma-1[22,23] were purchased from Immuno-Biological Laboratories Co. (Takasaki, Gunma, Japan) and were gifts from Dr. Noriyuki Masuda, Kinki Central Hospital, Sakai, Japan, respectively. Human dermal microvessel endothelial cell line (HMVEC) was purchased from Kurabo (Osaka, Japan). PC-9 and Ma-1 cell lines were maintained in RPMI 1640 medium supplemented with 10% fetal bovine serum (FBS), 100 U/mL of penicillin, 100 U/mL of streptomycin, and 2 mmol/L glutamine. HMVECs were maintained in HuMedia-MvG with growth supplements (Kurabo) and were used for *in vitro* assay at passages 2 to 5.

Reagents

E7050 was synthesized by Eisai Co. Ltd., Ibaraki, Japan[21] (see Supplemental Figure S1 at *http://ajp.amjpathol.org*). Its inhibitory concentration of 50% values for Met in MKN45 cells with amplified Met and for VEGFR-2 in human umbilical vein endothelial cells (HUVECs) were 14 and 16 nmol/L, respectively. In addition, oral administration of 25 mg/kg of E7050 inhibited Met phosphorylation and angiogenesis in xenograft tumors.[21] Gefitinib was obtained from AstraZeneca (Cheshire, UK). Recombinant HGF and anti-HGF Ab were prepared as reported previously.[24] The anti-VEGF Ab bevacizumab was obtained from Chugai Pharm (Tokyo, Japan). Recombinant VEGF, basic fibroblast growth factor, and epidermal growth factor (EGF) were obtained from R&D Systems (Minneapolis, MN).

Cell Growth Assay

Cell growth was measured using the MTT dye reduction method.[25] Tumor cells (2×10^3 cells/100 μL per well) were plated into each well of 96-well plates in RPMI1640 medium with 10% FBS. After 24-hour incubation, various reagents were added to each well and were incubated for a further 72 hours. HMVECs (5×10^3/200 μL per well) plated in 96-well plates precoated with 1.5% gelatin were incubated in M131 medium for 24 hours. Next, the cells were washed and incubated with various reagents for 72 hours in fresh minimal essential medium containing 5% FBS. Then, 50 μL of MTT solution (2 mg/mL; Sigma-Aldrich, St. Louis, MO) was added to all the wells, and incubation was continued for a further 2 hours. The media containing MTT solution were removed, and the dark blue crystals were dissolved by adding 100 μL of dimethyl sulfoxide. The absorbance was measured using a microplate reader at test and reference wavelengths of 550 and 630 nm, respectively. The percentage of growth is shown relative to untreated controls. Each experiment was performed at least in triplicate, and three times independently.

Antibodies and Western Blot Analysis

Cells were lysed in cell lysis buffer containing phosphatase inhibitor cocktail and proteinase inhibitor cocktail (Sigma-Aldrich), and the protein concentrations were determined using a Bicinchoninic Acid Protein Assay Kit (Pierce Biotechnology, Rockford, IL). Total protein (40 μg)

was resolved by SDS-PAGE (Bio-Rad Laboratories, Hercules, CA), and the proteins were then transferred onto polyvinylidene difluoride membranes (Bio-Rad Laboratories). After washing four times, membranes were incubated with Blocking One (Nacalai Tesque Inc., Kyoto, Japan) for 1 hour at room temperature and then were incubated overnight at 4°C with the following primary Abs: anti-Met (25H2), anti-phospho-Met (Y1234/Y1235) (3D7), anti-phospho-EGFR (Y1068), anti-ErbB3 (1B2), anti-phospho-ErbB3 (Tyr1289) (21D3), anti-Gab1 (#3232), phospho-Gab1 (Y627) (C32H2), anti-Akt, or phospho-Akt (Ser473) (736E11), anti-Shc1 (#2432) Abs (Cell Signaling Technology Inc., Beverly, MA) and anti-human EGFR (1 μg/mL) Ab (R&D Systems). After washing three times, membranes were incubated for 1 hour at room temperature with species-specific horseradish peroxidase–conjugated secondary Abs. Immunoreactive bands were visualized using SuperSignal west dura extended duration substrate enhanced chemiluminescent substrate (Pierce Biotechnology). Each experiment was performed at least three times independently.

Cytokine Production

Cells (2×10^5) were cultured in RPMI1640 medium with 10% FBS for 24 hours. The cells were washed with PBS and were incubated for 48 hours in 2 mL of RPMI1640 medium with 10% FBS. Then, culture medium was harvested and centrifuged, and the supernatant was stored at −70°C until analysis. The concentrations of HGF and VEGF were determined by IMMUNIS HGF enzyme immunoassay (Institute of Immunology, Tokyo, Japan) and Quantikine VEGF enzyme-linked immunosorbent assay (ELISA) (R&D Systems), respectively, according to the manufacturers' protocols. All the samples were run in duplicate. Color intensity was measured at 450 nm using a spectrophotometric plate reader. Growth factor concentrations were determined by comparison with standard curves. The detection limits for HGF and VEGF were 100 and 31 pg/mL, respectively.

HGF Gene Transfection

One day before transfection, aliquots of 1×10^5 Ma-1 cells in 1 mL of antibiotic-free medium were plated on 6-well plates. The full-length *HGF* cDNA cloned into the BCMGSneo expression vector[26] was transfected using Lipofectamine 2000 (Invitrogen, Carlsbad, CA) in accordance with the manufacturer's instructions. After 24-hour incubation, the cells were washed with PBS and then were incubated for an additional 72 hours in antibiotic-containing medium. Then, the cells were selected in G418 sulfate (Calbiochem, Jolla, CA). After limiting dilution, HGF-producing cells, Ma-1/HGF, were established. HGF production by Ma-1/HGF was confirmed by ELISA.

RNA Interference Assay

Duplexed Stealth RNAi (Invitrogen) against *MET*, *ErbB3*, *Gab1*, and *Shc1* and Stealth RNAi negative control low GC duplex #3 (Invitrogen) were used for RNA interference assay. One day before transfection, aliquots of 2×10^4 tumor cells in 400 μL of antibiotic-free medium were plated on 24-well plates. After incubation for 24 hours, the cells were transfected with small-interfering RNA (siRNA) (50 pmol) or scramble RNA using Lipofectamine 2000 (1 μL) in accordance with the manufacturer's instructions. After 24-hour incubation, the cells were washed with PBS and were incubated with or without various reagents for an additional 72 hours in antibiotic-containing medium. Cell growth was measured using a Cell Counting Kit-8 (Dojindo Molecular Technologies, Tokyo, Japan) in accordance with the manufacturer's instructions. Knockdown of *MET*, *ErbB3*, *Gab1*, and *Shc1* was confirmed by Western blot analysis. Each experiment was performed at least in triplicate and three times independently.

Xenograft Studies in Severe Combined Immunodeficiency Mice

Suspensions of Ma-1/Vec and Ma-1/HGF cells (3×10^6) were injected subcutaneously into the backs of 5-week-old female severe combined immunodeficiency (SCID) mice (Clea, Tokyo, Japan). After 7 days (tumors >5 mm in diameter), mice were randomly allocated into groups of 6 to 10 animals to receive E7050 (50 mg/kg per day) and/or gefitinib (25 mg/kg per day) by oral gavage. In some groups, anti-HGF neutralizing Ab (5 mg/kg per day) and/or anti-VEGF Ab (5 mg/kg three times a week) were injected i.p. The tumor volume was calculated (mm^3 = $width^2 \times length/2$). All the animal experiments complied with the Guidelines for the Institute for Experimental Animals, Kanazawa University Advanced Science Research Center.

Immunofluorescence for Phosphorylated VEGFR-2

To detect phosphorylated VEGFR-2 in HMVECs, HMVECs cultured on slides were rinsed with PBS and fixed in cold acetone for 5 minutes. After fixation, the slides were washed briefly in PBS and treated with 5% FBS for blocking. The slides were incubated with rabbit anti-phospho-VEGFR-2 Ab (Tyr1175, 19A10, 1:100 dilution; Cell Signaling Technology Inc.) at 4°C overnight. After washing, the slides were incubated with anti-rabbit Ab conjugated with Alexa Fluor 488 (green, 1:100 dilution; Invitrogen) and at room temperature for 40 minutes.

To detect CD31–phospho-VEGFR-2 double-positive endothelial cells, frozen sections (5 μm thick) of xenograft tumors were fixed with cold acetone and washed with PBS. After blocking with 5% normal horse serum, the slides were incubated overnight at 4°C with rabbit anti-phospho-VEGFR-2 Ab (Tyr1175) (19A10, 1:100 dilution) and rat anti-CD31 Ab (1:100 dilution; Pharmingen, San Diego, CA). After washing with PBS, the slides were stained with matched secondary Abs conjugated with Alexa Fluor 594 (red for CD31, 1:100) or Alexa Fluor 488 (green for phosphor VEGFR-2; 1:100 dilution). The localized green and red fluorescence were detected by fluorescence microscopy.

Immunohistochemical Analysis

Frozen sections (5 μm thick) of xenograft tumors were fixed with cold acetone and washed with PBS. After blocking the endogenous peroxidase activity with 3% aqueous H_2O_2 solution for 10 minutes, the sections were treated with 5% normal horse serum. The sections were then reacted with primary Ab (anti-CD31 Ab, 1:100 dilution) at 4°C overnight. After washing with PBS, anti-CD31 Ab–treated sections were incubated with peroxidase-conjugated anti-rat IgG for 40 minutes. The DAB (3,3′-diaminobenzidine tetrahydrochloride) liquid system (DakoCytomation, Glostrup, Denmark) was used to detect immunostaining. Omission of primary Ab served as a negative control.

Statistical Analysis

The statistical significance of differences was analyzed by one-way analysis of variance. In cases in which the *P* values for the overall comparisons were less than 0.05, post hoc pairwise comparisons were performed by the Newman-Keuls multiple comparison test. Statistical analyses were performed using GraphPad Prism software version 4.01 (GraphPad Software Inc., San Diego, CA).

Results

Met Inhibition Reverses Resistance to EGFR-TKIs Induced by Exogenous HGF

PC-9 and Ma-1 cells, which have an in-frame deletion in *EGFR* exon 19, were highly sensitive to gefitinib (Figure 1A).[11,23] None of these cell lines produced detectable levels of HGF protein (Figure 2A) or expressed T790M mutation in *EGFR* or amplified *Met*. As we reported previously, exogenously added HGF induced resistance to gefitinib in PC-9 and Ma-1 cells.[11,12] E7050, a dual TKI for Met and VEGFR-2, did not affect viability of PC-9 or Ma-1 cells at concentrations of <1 μmol/L. However, in combination with gefitinib, E7050 reversed HGF-induced resistance of PC-9 and Ma-1 cells in a dose-dependent manner (Figure 1B). These results indicated that E7050 could reverse EGFR-TKI resistance induced by exogenous HGF *in vitro*.

We next examined the effects of E7050 on signal transduction by Western blot analysis. Gefitinib inhibited the phosphorylation of EGFR and ErbB3 and, thereby, inhibited the phosphorylation of Akt and ERK1/2; however, gefitinib did not show this effect in the presence of HGF. E7050 suppressed constitutive phosphorylation of Met and its adaptor protein Gab1 but not EGFR, ErbB3, or downstream Akt and ERK1/2. HGF stimulated phosphorylation of Met and Gab1. E7050 successfully inhibited HGF-induced phosphorylation of Met and Gab1 and strongly suppressed phosphorylation of Akt combined with gefitinib (Figure 1C).

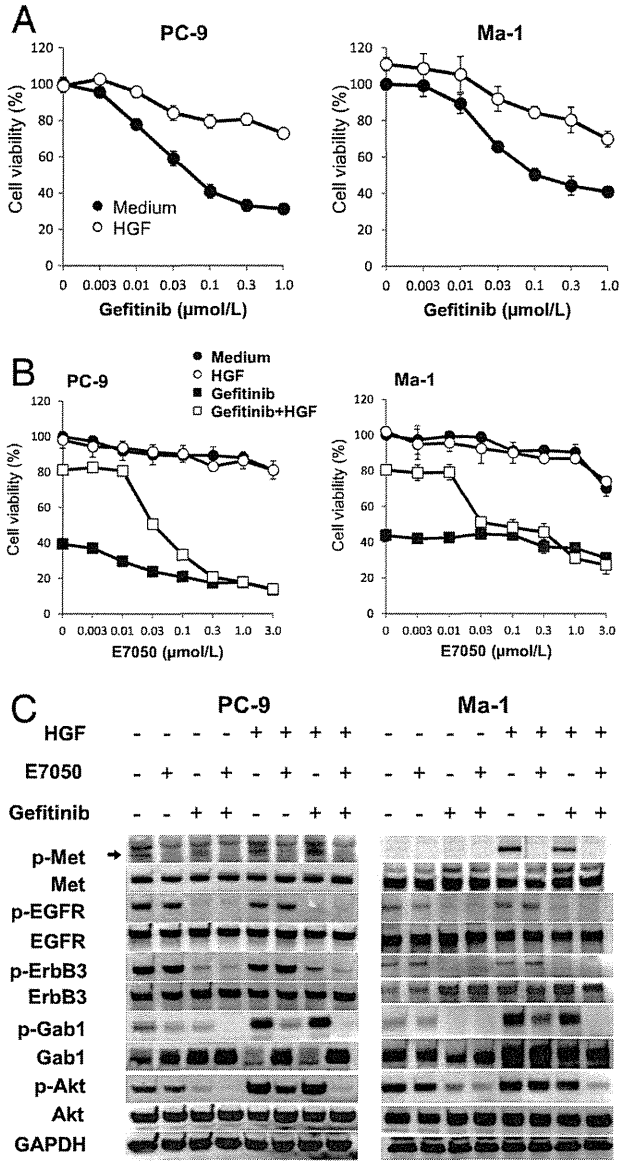

Figure 1. Met inhibition by E7050 overcomes resistance to EGFR-TKIs induced by exogenous HGF. **A:** PC-9 and Ma-1 cells were incubated with various concentrations of gefitinib with or without HGF (20 ng/mL). Cell growth was determined by MTT assay. Error bars indicate SD. **B:** PC-9 and Ma-1 cells were incubated with various concentrations of E7050 with or without HGF (20 ng/mL) and/or gefitinib (0.3 μmol/L). Cell growth was determined by MTT assay. **C:** PC-9 and Ma-1 cells were incubated with E7050 (1 μmol/L) and/or gefitinib (1 μmol/L) for 1 hour. Then, HGF (20 ng/mL) was added. Ten minutes later, cell lysates were harvested, and phosphorylation of the indicated proteins was determined by Western blot analysis. GAPDH, glyceraldehyde-3-phosphate dehydrogenase.

Met Inhibition Overcomes Resistance to EGFR-TKIs Induced by Endogenous HGF

A previous study demonstrated that HGF is mainly detected in cancer cells in patients with non–small-cell lung cancer and acquired resistance to EGFR-TKIs and that transient HGF gene transfection into PC-9 cells resulted in resistance to EGFR-TKIs.[11] Herein, we further generated stable HGF gene transfectants (Ma-1/HGF) using Ma-1 cells to assess the role of continuously produced endogenous HGF. Ma-1/Vec were used as control cells

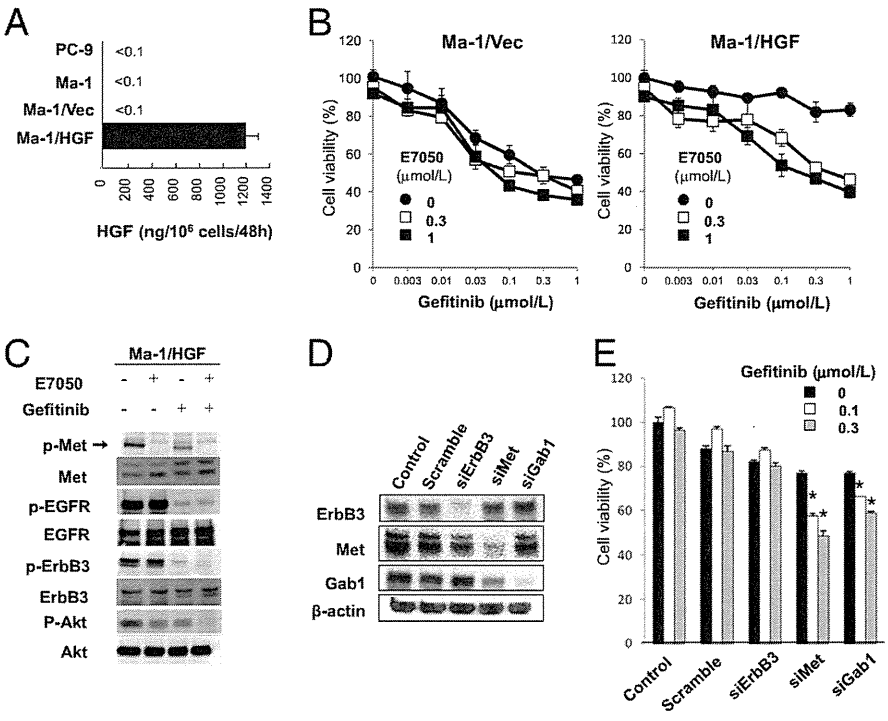

Figure 2. Met inhibition by E7050 overcomes resistance to EGFR-TKIs induced by endogenous HGF. **A:** Tumor cells (1×10^6/10 mL) were incubated for 48 hours. Concentration of HGF in the culture supernatants was determined by ELISA. **B:** Ma-1/Vec and Ma-1/HGF cells were incubated with various concentrations of gefitinib with or without E7050. Cell growth was determined by MTT assay. **C:** Ma-1/HGF cells were incubated with E7050 (1 μmol/L) and/or gefitinib (1 μmol/L) for 1 hour. Then, cell lysates were harvested, and phosphorylation of the indicated proteins was determined by Western blot analysis. **D:** Ma-1/HGF cells were treated with or without scramble, *ErbB3*, *Met*, or *Gab1* siRNA for 12 hours and were further incubated in medium for 48 hours. Then, cell lysates were harvested, and expression of the indicated proteins was determined by Western blot analysis. **E:** Ma-1/HGF cells were treated with siRNA as in **D**. After 72-hour incubation in medium, cell growth was determined by MTT assay. $^*P < 0.05$ versus medium alone (one-way ANOVA). Bars indicate SD.

transfected with vector alone. Ma-1/HGF, but not Ma-1 or Ma-1/Vec, secreted high levels of HGF and became resistant to gefitinib (Figure 2, A and B). Anti-HGF Ab reversed gefitinib resistance of Ma-1/HGF cells (data not shown), indicating that endogenously produced HGF induced gefitinib resistance in this cell line. E7050 combined with gefitinib successfully reversed resistance of Ma-1/HGF cells, whereas E7050 alone did not markedly inhibit the viability of Ma-1/HGF cells (Figure 2B). Gefitinib inhibited phosphorylation of EGFR and ErbB3 in Ma-1/HGF cells but did not inhibit phosphorylation of Akt. E7050 inhibited phosphorylation of Met and Gab1 and suppressed phosphorylation of Akt in combination with gefitinib (Figure 2C).

To confirm that reversal of gefitinib resistance by E7050 in Ma-1/HGF cells is due to inhibition of Met/Gab1, we conducted experiments with siRNA specific for *Met* or *Gab1*. Treatment with siRNA for *ErbB3*, *Met*, and *Gab1* successfully knocked down the corresponding protein expression (Figure 2D). Scramble or *ErbB3* siRNA did not reverse gefitinib resistance of Ma-1/HGF cells. However, siRNA for *Met* and siRNA for *Gab1* considerably sensitized Ma-1/HGF cells to gefitinib, indicating that E7050 reverses gefitinib resistance in Ma-1/HGF cells by inhibiting the Met/Gab1 pathway.

Antiangiogenic Effect of E7050 by Inhibition of VEGFR-2

We next explored the potential of E7050 against VEGFR-2. Western blot analysis indicated that HMVECs expressed VEGFR-2 protein at high levels, whereas the human *EGFR* mutant lung cancer cell lines PC-9, Ma-1, Ma-1/Vec, and Ma-1/HGF did not (Figure 3A). VEGFR-2 was phosphorylated by VEGF stimulation in HMVECs, and E7050 showed an inhibitory effect (Figure 3, B and C). E7050 slightly inhibited constitutive viability of HMVEC cells (Figure 3D). HMVEC growth was stimulated by VEGF and basic fibroblast growth factor but not by HGF or EGF. E7050 inhibited VEGF-stimulated HMVEC growth in a dose-dependent manner (Figure 3D). E7050 was less effective against basic fibroblast growth factor–stimulated HMVEC growth. These results indicated selective activity of E7050 against VEGF–VEGFR-2.

HGF Stimulates VEGF Production by EGFR *Mutant Lung Cancer Cells and E7050 Shows an Inhibitory Effect*

PC-9 and Ma-1 cells constitutively produced detectable levels of VEGF, and HGF stimulated VEGF production (Figure 4A). Consistent with these observations, Ma-1/HGF cells produced higher levels of VEGF (mean ± SD) than did Ma-1/Vec cells (2110 ± 40 versus 1170 ± 50 pg/10^6 per 48 hours). As HGF was reported to enhance VEGF production mediated by Shc1, an adaptor protein for Met, in endothelial cells,[27] we next evaluated the involvement of Shc1 compared with Gab1, a common adaptor of Met, using specific siRNA. Treatment with siRNA for *Met*, *Shc1*, and *Gab1* successfully knocked down expression of the corresponding protein (Figure 2D; see also Supplemental Figure S2 at *http://ajp.amjpathol.org*). Silencing of *Met* and *Gab1*, but not *Shc1*, canceled the augmented VEGF production by HGF, indicating that HGF stimulates VEGF production by activating Met predominantly using Gab1, not Shc1, as an adaptor (Figure 4B). Moreover, E7050 successfully canceled HGF-induced VEGF production (Figure 4C). Immunoblotting with immunoprecipitation showed that

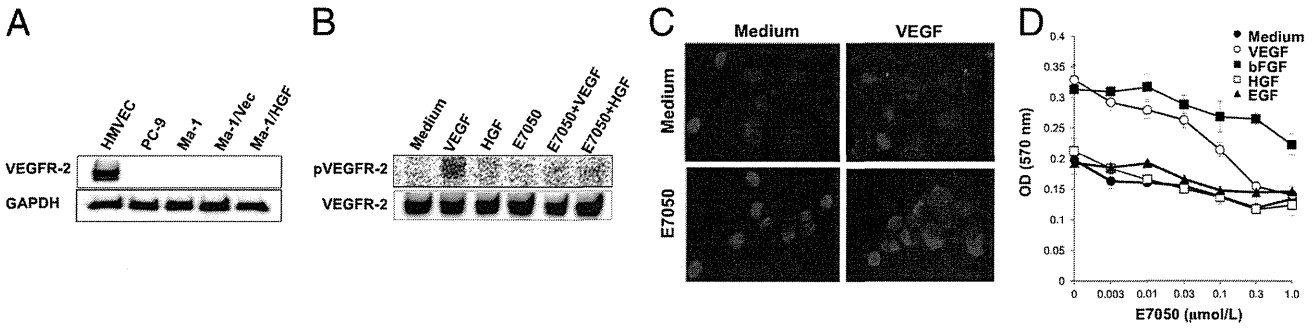

Figure 3. E7050 inhibits VEGFR-2 phosphorylation and suppresses growth of HMVECs. **A:** VEGFR-2 protein expression in HMVEC and *EGFR* mutant lung cancer cell lines was examined by Western blot analysis. GAPDH, glyceraldehyde-3-phosphate dehydrogenase. **B:** HMVECs were cultured with or without E7050 (1 μmol/L) for 1 hour, and then 50 ng/mL of VEGF and HGF were added. After 10 minutes, the cells were lysed, and the indicated proteins were detected by immunoblotting. **C:** HMVECs were cultured with or without E7050 (1 μmol/L) for 1 hour, and then VEGF was added. After 10 minutes, the cells were fixed and stained for phosphorylated VEGFR-2. Phosphorylated VEGFR-2 was detected on the plasma membrane after VEGF stimulation. E7050 prevented expression of phosphorylated VEGFR-2 even after VEGF stimulation. **D:** HMVECs were incubated with various concentrations of E7050 for 72 hours with or without 50 ng/mL of VEGF, basic fibroblast growth factor (bFGF), HGF, or EGF. Cell growth was determined by MTT assay. Bars indicate SD.

Gab1 was constitutively associated with Met and weakly phosphorylated in Ma-1 cells. HGF remarkably augmented phosphorylation of Gab1 associated with Met (Figure 4D). Although E7050 did not affect constitutive association between Met and Gab1, it inhibited HGF-induced Gab1 phosphorylation (Figure 4D). These findings indicated that Gab1 constitutively associates with Met and mediates important signaling for not only induction of EGFR-TKI resistance but also stimulation of VEGF production.

E7050 Circumvents HGF-Induced Resistance When Combined with Gefitinib in Vivo

To investigate the therapeutic efficacy of E7050, we inoculated Ma-1/Vec or Ma-1/HGF cells into SCID mice subcutaneously. Gefitinib treatment (25 mg/kg) induced regression of tumors formed by Ma-1/Vec cells, and E7050 treatment (50 mg/kg) showed a slight inhibitory effect (Figure 5A). Under these experimental conditions, gefitinib treatment inhibited the growth of Ma-1/HGF tumors only marginally, indicating gefitinib resistance *in vivo* caused by endogenous HGF (Figure 5B). E7050 treatment alone also retarded tumor growth, indicating mild antitumor activity of E7050 as monotherapy. However, E7050 combined with gefitinib resulted in marked growth regression of Ma-1/HGF tumors (Figure 5B).

Western blot analyses using *in vivo* tumors indicated that phosphorylation of Akt, an important survival signaling in *EGFR* mutant lung cancer, was inhibited only by combined treatment with gefitinib and E7050 in Ma-1/HGF tumors (Figure 5C; see also Supplemental Figure S3 at *http://ajp.amjpathol.org*). Histologic examinations showed that tumors produced by HGF-transfected Ma-1 (Ma-1/HGF) cells were more angiogenic than those produced by Ma-1/Vec cells (see Supplemental Figure S4 at *http://ajp.amjpathol.org*). In Ma-1/HGF tumors, wh-

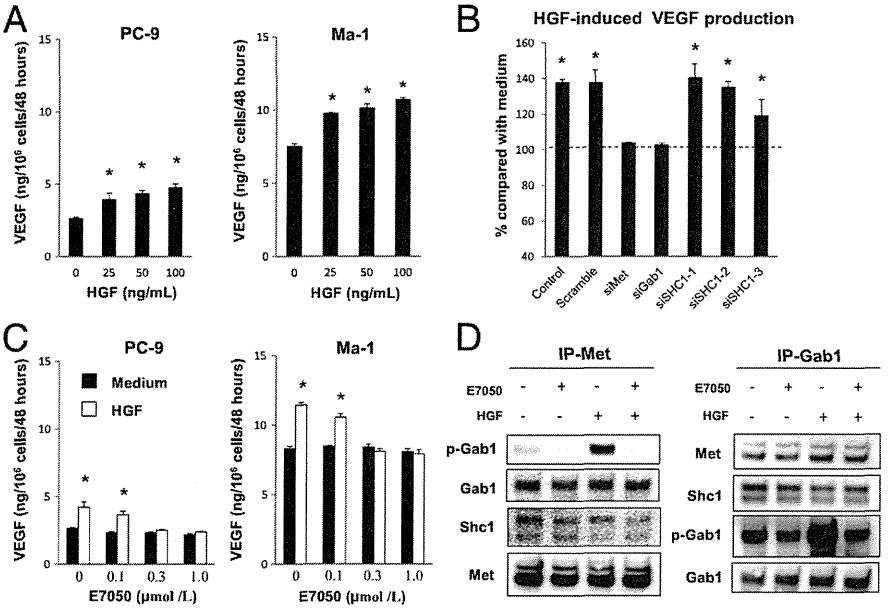

Figure 4. HGF stimulates VEGF production by *EGFR* mutant lung cancer cells. **A:** PC-9 and Ma-1 cells (2×10^5/2 mL) were incubated with or without HGF for 48 hours. Concentration of VEGF in the culture supernatants was determined by ELISA. $^*P < 0.05$ versus medium alone. Bars indicate SD. **B:** Ma-1 cells were treated with scramble, *Met*, *Gab1*, or *Shc1* siRNA for 12 hours and then were further incubated in medium for 48 hours. Then, the concentration of VEGF in the culture supernatants was determined by ELISA. $^*P < 0.05$ versus *siMet*. **C:** PC-9 and Ma-1 cells (2×10^5/2 mL) were incubated with or without HGF (50 ng/mL) in the presence or absence of E7050 (1 μmol/L) for 48 hours. Concentration of VEGF in the culture supernatants was determined by ELISA. $^*P < 0.05$ versus medium. **D:** Ma-1 cells were incubated with or without E7050 (1 μmol/L) for 1 hour and then were further incubated with or without HGF (50 ng/mL) for 10 minutes. Then, cell lysates were harvested and immunoprecipitated with the indicated antibody. Protein association was determined by Western blot analysis.

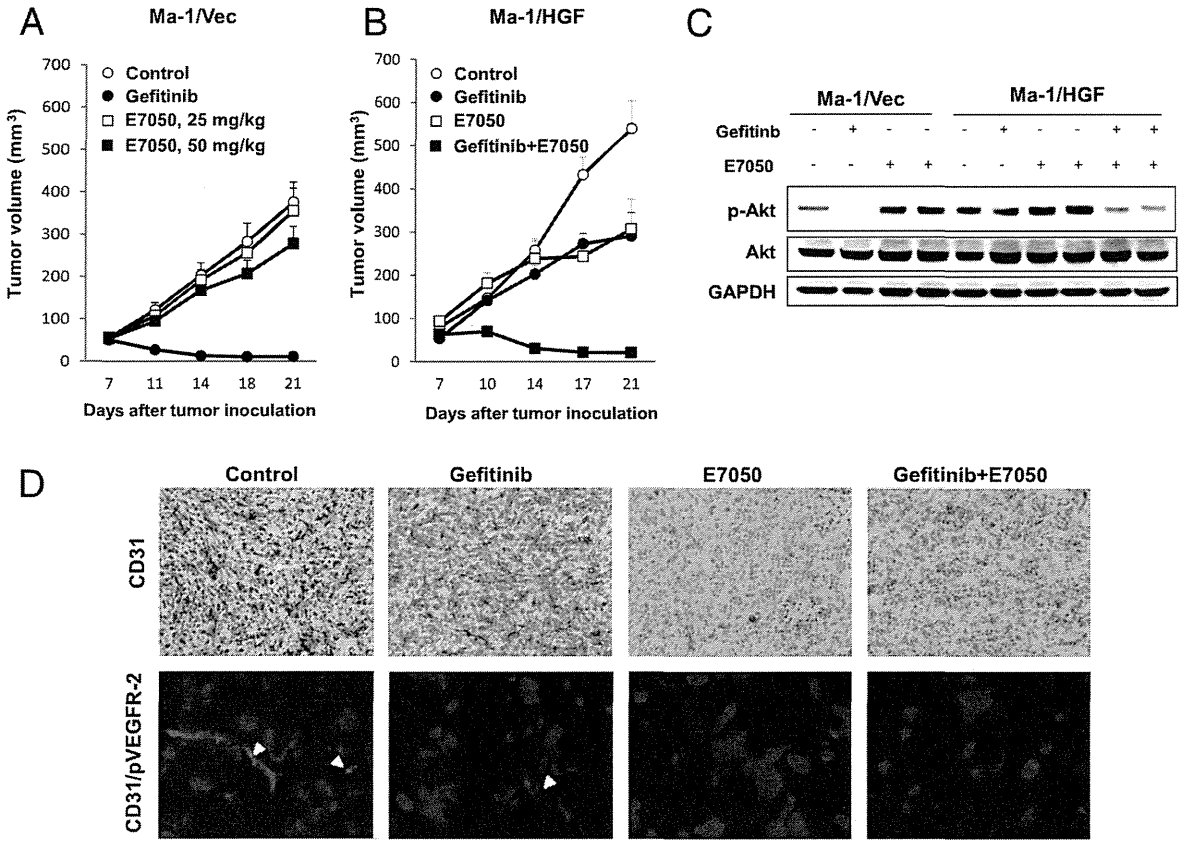

Figure 5. E7050 circumvents HGF-induced resistance *in vivo* when combined with gefitinib. **A:** Ma-1/Vec cells (3×10^6) were inoculated s.c. into SCID mice. Oral treatment with E7050 (25 or 50 mg/kg) or gefitinib (25 mg/kg) was given daily from day 7. Data shown are the mean ± SE of six tumors. **B:** Ma-1/HGF cells (3×10^6) were inoculated s.c. into SCID mice. Oral treatment with E7050 (50 mg/kg) and/or gefitinib (25 mg/kg) was given daily from day 7. Data shown are the mean ± SE of six tumors. **C:** Tumors harvested on day 21 were lysed and examined for phosphorylated Akt by Western blot analysis. GAPDH, glyceraldehyde-3-phosphate dehydrogenase. **D:** Ma-1/HGF-bearing SCID mice were treated with E7050 (50 mg/kg) and/or gefitinib (25 mg/kg) for 5 days. The tumors were harvested, and frozen sections were examined for endothelial cells (CD31) and phosphorylated VEGFR-2 (pVEGFR-2) by immunostaining. **Arrowheads** indicate endothelial cells. Numbers of CD31-positive endothelial cells in a field (×200) are also shown.

ereas gefitinib treatment did not affect the number of CD31-positive endothelial cells, E7050 with or without gefitinib dramatically inhibited the number of CD31-positive endothelial cells (Figure 5D; see also Supplemental Figure S5 at *http://ajp.amjpathol.org*), indicating potent antiangiogenic efficacy of E7050.

Moreover, control- or gefitinib-treated tumor contained CD31–phosphorylated VEGFR-2 double-positive cells but not in tumors treated with E7050 alone or gefitinib+E7050 (Figure 5D), indicating an association between antiangiogenic effect of E7050 and inhibition of VEGFR-2 phosphorylation *in vivo*. We also assessed the effects of gefitinib and/or E7050 on cell proliferation (Ki-67) and apoptosis (TUNEL). We found that gefitinib with or without E7050 suppressed cell proliferation in Ma-1/Vec tumors, whereas E7050 alone did not (see Supplemental Figures S5 and S6 at *http://ajp.amjpathol.org*). In Ma-1/HGF tumors, monotherapy with gefitinib or E7050 tended to reduce the number of proliferating cells, whereas combination treatment markedly inhibited cell proliferation. The number of apoptotic cells was increased in Ma-1/Vec tumors treated with gefitinib or E7050 and was markedly increased in tumors treated with both (see Supplemental Figures S5 and S7 at *http://ajp.amjpathol.org*). The number of apoptotic cells in Ma-1/HGF tumors was increased by E7050, unaffected by gefitinib, and markedly increased by combined gefitinib and E7050. These results suggest that monotherapy with the angiogenesis inhibitor E7050 was not sufficient for regressing Ma-1/HGF tumors, whereas its combination with gefitinib, which blocks EGFR signaling, was necessary for tumor regression.

Dual Inhibition of HGF and VEGF by Specific Abs Reverses HGF-Induced Resistance When Combined with Gefitinib in Vivo

To confirm the effects of dual targeting of HGF/Met and VEGF/VEGFR-2 on HGF-induced resistance, we finally examined the effects of anti-HGF Ab and anti-VEGF Ab with gefitinib against Ma-1/HGF tumors *in vivo*. Anti-HGF Ab and gefitinib slightly inhibited the growth of Ma-1/HGF tumors (Figure 6A). However, combined use of anti-HGF Ab and gefitinib further inhibited the growth, suggesting that anti-HGF Ab neutralized HGF and resensitized Ma-1/HGF cells to gefitinib *in vivo* (Figure 6A). In a parallel experiment, monotherapy with anti-VEGF Ab or combined treatment with anti-HGF Ab and anti-VEGF Ab inhibited tumor growth as effectively as com-

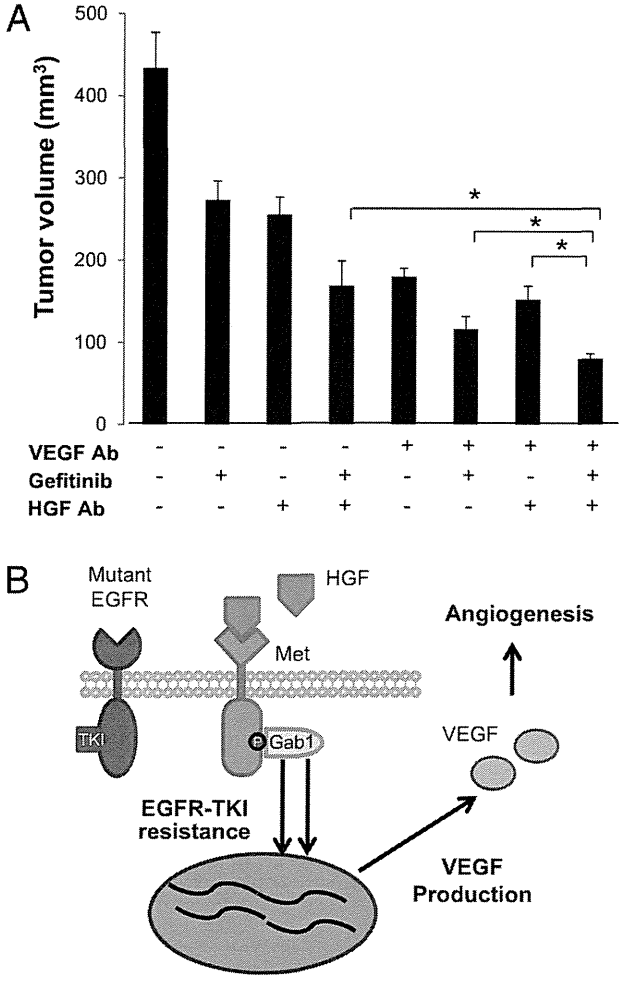

Figure 6. Dual inhibition of HGF and VEGF by specific antibodies reversed HGF-induced resistance when combined with gefitinib *in vivo*. **A:** Ma-1/HGF cells (3×10^6) were inoculated subcutaneously into SCID mice. From day 7, oral daily treatment with gefitinib (25 mg/kg), i.p. daily treatment with anti-HGF Ab (5 mg/kg per day), and/or i.p. treatment with anti-VEGF Ab (5 mg/kg per day, three times a week), were given. Data shown are the mean ± SE of six tumors on day 17. $^*P < 0.05$. Bars indicate SD. **B:** Scheme showing the role of HGF in *EGFR* mutant lung cancer cells. HGF induces EGFR-TKI resistance and VEGF production by activating the Met/Gab1 axis.

bined treatment with anti-HGF Ab and gefitinib in this model. The addition of gefitinib to anti-VEGF Ab further inhibited growth. Combined use of anti-HGF Ab, anti-VEGF Ab, and gefitinib showed the strongest inhibitory effect on the growth of Ma-1/HGF tumors, indicating the usefulness of dual inhibition of HGF and VEGF for overcoming HGF-induced resistance to EGFR-TKIs (Figure 6A). This was further supported by results of histologic analysis with Ma-1/HGF tumors. Anti-HGF Ab tended to decrease the number of proliferating tumor cells and tumor vessels and increase the number of apoptotic cells (see Supplemental Figures S5–S8 at *http://ajp.amjpathol.org*). Anti-HGF Ab with gefitinib discernibly reduced proliferating cell numbers, tumor vessel numbers, and phosphorylation of Akt and increased apoptotic cell numbers, but their effects were less than those of E7050 (dual inhibitor of HGF/Met and VEGFR-2) with gefitinib.

Discussion

HGF is a mediator that regulates multiple biological functions, including cell motility, invasion, and angiogenesis.[28] Moreover, recent studies indicated considerable roles of HGF on sensitivity to anticancer agents. For example, HGF was reported to induce cisplatin resistance in lung adenocarcinoma cells by reducing the expression of apoptosis-inducing factor.[29] It inhibited Fas-induced apoptosis by activating the PI3K/Akt pathway and, thus, inhibiting Fas death-inducing signaling complex formation in hepatocellular carcinoma.[30] HGF also suppressed anoikis by increasing cyclooxygenase-2 expression through activation of Erk and AP-1 in head and neck squamous cell carcinoma.[31] Regarding sensitivity to molecularly targeted drugs, we demonstrated that HGF induces EGFR-TKI resistance in *EGFR* mutant lung cancer.[11] Thus, accumulating evidence suggests that HGF is an ideal therapeutic target for drug resistance in various types of cancer.

In the present study, we found that HGF stimulates VEGF production of *EGFR* mutant lung cancer cells by predominantly activating the Met/Gab1 axis in the same way as induction of EGFR-TKI resistance (Figure 6B). Moreover, the present findings using mainly E7050, a dual inhibitor of Met and VEGFR-2 kinases, indicated the rationale of dual inhibition of the HGF-Met axis and the VEGF-VEGFR-2 axis on treatment of HGF-induced EGFR-TKI resistance in *EGFR* mutant lung cancer. This strategy was supported by recent studies indicating that blockade of VEGFR signaling caused hypoxia by inhibition of angiogenesis and that hypoxia is likely to enhance HGF-Met signaling and, thereby, promote tumor survival and metastasis. In fact, in renal cell carcinoma, HGF was reported to induce resistance to sunitinib, an inhibitor of multiple kinases, including VEGFR-2, by compensating for inhibited angiogenesis.[32] In a model of pancreatic neuroendocrine cancer, inhibition of VEGFR caused shrinkage of the primary tumor, but it also made the surviving cancer more aggressive with more metastatic behavior.[33] Clinical studies indicated a correlation between the presence of hypoxic regions in neoplastic lesions and poor prognosis.[34] Hypoxic conditions induced transcriptional activation of Met and subsequent amplification of HGF-Met signaling, thereby increasing the invasiveness of cancer cells.[35] Therefore, dual blockade of the HGF-Met and VEGF-VEGFR axes may be valuable for overcoming not only EGFR-TKI resistance but also angiogenesis inhibitor resistance.

In endothelial cells, HGF was reported to induce VEGF production using Shc1 as an adaptor for Met.[27] In contrast, silencing of *Shc1* did not abrogate HGF-induced VEGF production in *EGFR* mutant lung cancer cells, although similar to Gab1, Shc1 constitutively associated with Met, as well as with Gab1. On the other hand, Gab1 is thought to be an important adaptor protein for Met-mediating signaling in various cell types. The present data show that Gab1 constitutively associated with Met and HGF markedly stimulated phosphorylation of Gab1 in *EGFR* mutant lung cancer cells. Silencing of Gab1 successfully canceled HGF-stimulated VEGF production and

HGF-induced EGFR-TKI resistance. These findings suggest that Gab1 may be a novel ideal target for controlling *EGFR* mutant lung cancer.

These data suggest that E7050 regressed tumors with HGF-induced resistance by several mechanisms. First, E7050 inhibited phosphorylation of Met expressed in cancer cells, blocked the downstream Gab1/PI3K/Akt pathway, and, hence, resensitized the cancer cells. Second, E7050 inhibited HGF-induced VEGF production by cancer cells and may indirectly suppress angiogenesis. Third, E7050 inhibited phosphorylation of VEGFR-2 in endothelial cells and directly suppressed angiogenesis. VEGF inhibition was suggested to normalize tumor vascular structure and permeability, decrease tumor interstitial pressure, and increase penetration of anticancer drugs into tumors.[36] Therefore, it is also possible that E7050 increased its own penetration into tumors by inhibiting VEGFR-2 phosphorylation and normalizing tumor vascular structure and permeability. Recently, neuropilin-1, the co-receptor for VEGF165 isoform, was reported to associate with Met and to mediate VEGF-triggered expression of myeloid cell leukemia-1, a member of the Bcl-2 family, which inhibits cell apoptosis, in prostate cancer cells.[37] In Ma-1/HGF tumors, E7050 treatment decreased the expression of myeloid cell leukemia-1 and survivin, another member of the Bcl family (see Supplemental Figure S9 at *http://ajp.amjpathol.org*). Thus, E7050 might also inhibit VEGF/neuropilin–triggered antiapoptotic protein expression by suppressing Met phosphorylation.

A recent study indicated an interaction between HGF and *Met* amplification in EGFR-TKI resistance in lung cancer. In the presence of gefitinib, continuous exposure to HGF accelerates expansion of preexisting *MET*-amplified cancer cells, although this was observed only in HCC827 cells.[13] We established Ma-1 cells (Ma-1/HGF) constitutively producing HGF by *HGF* gene transfection. However, Ma-1/HGF did not show *Met* amplification (data not shown). Therefore, this phenomenon may be uniquely observed in a population of *EGFR* mutant lung cancer cells.

It is important to define the incidence rate of HGF-induced resistance to EGFR-TKI in *EGFR* mutant lung cancer. In a previous study with 10 clinical specimens of *EGFR* mutant lung cancer, we reported the presence of patients whose resistance was associated with high HGF expression but not *EGFR*-T790M second mutation or *Met* amplification.[11] This was confirmed by another group.[13] Moreover, it was reported that HGF is frequently co-expressed in tumors with *EGFR*-T790M secondary mutation or *Met* amplification.[13,15] Although there are considerable ethnic differences in the incidence rates of *EGFR* mutation in lung cancer,[38] it is still unclear whether there are ethnic differences in the incidence of resistance mechanisms, such as *EGFR*-T790M secondary mutation, *Met* amplification, and HGF overexpression. We are currently engaged in a multicenter trial to elucidate the incidence of HGF-induced EGFR-TKI resistance and the involvement of angiogenesis in a Japanese cohort. Recent studies indicated that blood levels of HGF and/or VEGF are associated with clinical response to EGFR-TKIs in patients with lung cancer,[39–41] suggesting key roles of HGF and VEGF and the possibility of noninvasive diagnosis of HGF-induced resistance to EGFR-TKIs.

In conclusion, we provided preclinical evidence showing the rationale of dual inhibition of HGF-Met and VEGF-VEGFR-2 in HGF-induced EGFR-TKI resistance of *EGFR* mutant lung cancer. Further studies are needed to determine whether dual targeting therapy will be clinically effective in patients with *EGFR* mutant lung cancer who develop HGF-induced resistance.

Acknowledgment

We thank Dr. Naofumi Mukaida (Cancer Research Institute, Kanazawa University, Kanazawa, Japan) for providing BCMGSneo plasmid.

References

1. Herbst RS, Heymach JV, Lippman SM: Lung cancer. N Engl J Med 2008, 359:1367–1380
2. Lynch TJ, Bell DW, Sordella R, Gurubhagavatula S, Okimoto RA, Brannigan BW, Harris PL, Haserlat SM, Supko JG, Haluska FG, Louis DN, Christiani DC, Settleman J, Haber DA: Activating mutations in the epidermal growth factor receptor underlying responsiveness of non-small-cell lung cancer to gefitinib. N Engl J Med 2004, 350:2129–2139
3. Paez JG, Jänne PA, Lee JC, Tracy S, Greulich H, Gabriel S, Herman P, Kaye FJ, Lindeman N, Boggon TJ, Naoki K, Sasaki H, Fujii Y, Eck MJ, Sellers WR, Johnson BE, Meyerson M: EGFR mutations in lung cancer: correlation with clinical response to gefitinib therapy. Science 2004, 304:1497–1500
4. Sandler A, Gray R, Perry MC, Brahmer J, Schiller JH, Dowlati A, Lilenbaum R, Johnson DH: Paclitaxel-carboplatin alone or with bevacizumab for non-small-cell lung cancer. N Engl J Med 2006, 355: 2542–2550
5. Mitsudomi T, Morita S, Yatabe Y, Negoro S, Okamoto I, Tsurutani J, Seto T, Satouchi M, Tada H, Hirashima T, Asami K, Katakami N, Takada M, Yoshioka H, Shibata K, Kudoh S, Shimizu E, Saito H, Toyooka S, Nakagawa K, Fukuoka M: Gefitinib versus cisplatin plus docetaxel in patients with non-small-cell lung cancer harbouring mutations of the epidermal growth factor receptor (WJTOG3405): an open label, randomised phase 3 trial. Lancet Oncol 2010, 11:121–128
6. Maemondo M, Inoue A, Kobayashi K, Sugawara S, Oizumi S, Isobe H, Gemma A, Harada M, Yoshizawa H, Kinoshita I, Fujita Y, Okinaga S, Hirano H, Yoshimori K, Harada T, Ogura T, Ando M, Miyazawa H, Tanaka T, Saijo Y, Hagiwara K, Morita S, Nukiwa T: Gefitinib or chemotherapy for non-small-cell lung cancer with mutated EGFR. N Engl J Med 2010, 362:2380–2388
7. Jackman D, Pao W, Riely GJ, Engelman JA, Kris MG, Jänne PA, Lynch T, Johnson BE, Miller VA: Clinical definition of acquired resistance to epidermal growth factor receptor tyrosine kinase inhibitors in non-small-cell lung cancer. J Clin Oncol 2010, 28:357–360
8. Kobayashi S, Boggon TJ, Dayaram T, Jänne PA, Kocher O, Meyerson M, Johnson BE, Eck MJ, Tenen DG, Halmos B: EGFR mutation and resistance of non-small-cell lung cancer to gefitinib. N Engl J Med 2005, 352:786–792
9. Pao W, Miller VA, Politi KA, Riely GJ, Somwar R, Zakowski MF, Kris MG, Varmus H: Acquired resistance of lung adenocarcinomas to gefitinib or erlotinib is associated with a second mutation in the EGFR kinase domain. PLoS Med 2005, 2:e73
10. Engelman JA, Zejnullahu K, Mitsudomi T, Song Y, Hyland C, Park JO, Lindeman N, Gale CM, Zhao X, Christensen J, Kosaka T, Holmes AJ, Rogers AM, Cappuzzo F, Mok T, Lee C, Johnson BE, Cantley LC, Jänne PA: MET amplification leads to gefitinib resistance in lung cancer by activating ERBB3 signaling. Science 2007, 316:1039–1043
11. Yano S, Wang W, Li Q, Matsumoto K, Sakurama H, Nakamura T, Ogino H, Kakiuchi S, Hanibuchi M, Nishioka Y, Uehara H, Mitsudomi

T, Yatabe Y, Nakamura T, Sone S: Hepatocyte growth factor induces gefitinib resistance of lung adenocarcinoma cells with EGF receptor mutations. Cancer Res 2008, 68:9479–9487
12. Wang W, Li Q, Yamada T, Matsumoto K, Matsumoto I, Oda M, Watanabe G, Kayano Y, Nishioka Y, Sone S, Yano S: Crosstalk to stromal fibroblasts induces resistance of lung cancer to EGFR tyrosine kinase inhibitors. Clin Cancer Res 2009, 15:6630–6638
13. Turke AB, Zejnullahu K, Wu YL, Song Y, Dias-Santagata D, Lifshits E, Toschi L, Rogers A, Mok T, Sequist L, Lindeman NI, Murphy C, Akhavanfard S, Yeap BY, Xiao Y, Capelletti M, Iafrate AJ, Lee C, Christensen JG, Engelman JA, Jänne PA: Preexistence and clonal selection of MET amplification in EGFR mutant NSCLC. Cancer Cell 2010, 17:77–88
14. Yamada T, Matsumoto K, Wang W, Li Q, Nishioka Y, Sekido Y, Sone S, Yano S: Hepatocyte growth factor reduces susceptibility to an irreversible epidermal growth factor receptor inhibitor in EGFR-T790M mutant lung cancer. Clin Cancer Res 2010, 16:174–183
15. Onitsuka T, Uramoto H, Nose N, Takenoyama M, Hanagiri T, Sugio K, Yasumoto K: Acquired resistance to gefitinib: the contribution of mechanisms other than the T790M. MET, and HGF status. Lung Cancer 2010, 68:198–203
16. Miller VA, Hirsh V, Cadranel J, Chen Y-M, Park K, Kim SW, Caicun Z, Oberdick M, Shahidi M, Yang CH: Phase IIb/III double-blind randomized trial of afatinib (BIBW2992, and irreversible inhibitor of EGFR/HER1 and Her2) + best supportive care (BSC) versus placebo + BSC in patients with NSCLC failing 1–2 lines of chemotherapy and erlotinib or gefitinib (LUX-Lung 1) (abstract LBA1). Ann Oncol 2010, 21:viii1
17. Sequist LV, Besse B, Lynch TJ, Miller VA, Wong KK, Gitlitz B, Eaton K, Zacharchuk C, Freyman A, Powell C, Ananthakrishnan R, Quinn S, Soria JC: Neratinib, an irreversible pan-ErbB receptor tyrosine kinase inhibitor: results of a phase II trial in patients with advanced non-small-cell lung cancer. J Clin Oncol 2010, 28:3076–3083
18. Keedy VL, Sandler AB: Inhibition of angiogenesis in the treatment of non-small cell lung cancer. Cancer Sci 2007, 98:1825–1830
19. Dong G, Lee TL, Yeh NT, Geoghegan J, Waes CV, Chen Z: Metastatic squamous cell carcinoma cells that overexpress c-Met exhibit enhanced angiogenesis factor expression, scattering and metastasis in response to hepatocyte growth factor. Oncogene 2004, 23:6199–6208
20. Van Belle E, Witzenbichler B, Chen D, Silver M, Chang L, Schwall R, Isner JM: Potentiated angiogenic effect of scatter factor/hepatocyte growth factor via induction of vascular endothelial growth factor: the case for paracrine amplification of angiogenesis. Circulation 1998, 97:381–390
21. Nakagawa T, Tohyama O, Yamaguchi A, Matsushima T, Takahashi K, Funasaka S, Shirotori S, Asada M, Obaishi H: E7050: a dual c-Met and VEGFR-2 tyrosine kinase inhibitor promotes tumor regression and prolongs survival in mouse xenograft models. Cancer Sci 2010, 101:210–215
22. Masuda N, Fukuoka M, Matsui K, Kusunoki Y, Kudoh S, Negoro S, Takifuji N, Fujisue M, Morino H, Nakagawa K, Nishioka M, Takada M: Establishment of tumor cell lines as an independent prognostic factor for survival time in patients with small-cell lung cancer. J Natl Cancer Inst 1991, 83:1743–1748
23. Okabe T, Okamoto I, Tamura K, Terashima M, Yoshida T, Satoh T, Takada M, Fukuoka M, Nakagawa K: Differential constitutive activation of the epidermal growth factor receptor in non-small cell lung cancer cells bearing EGFR gene mutation and amplification. Cancer Res 2007, 67:2046–2053
24. Montesano R, Matsumoto K, Nakamura T, Orci L: Identification of a fibroblast-derived epithelial morphogen as hepatocyte growth factor. Cell 1991, 67:901–908
25. Green LM, Reade JL, Ware CF: Rapid colorimetric assay for cell viability: application to the quantitation of cytotoxic and growth inhibitory lymphokines. J Immunol Methods 1984, 70:257–268
26. Nishioka Y, Yano S, Fujiki F, Mukaida N, Matsushima K, Tsuruo T, Sone S: Combined therapy of multidrug-resistant human lung cancer with anti-P-glycoprotein antibody and monocyte chemoattractant protein-1 gene transduction: the possibility of immunological overcoming of multidrug resistance. Int J Cancer 1997, 71:170–177
27. Saucier C, Khoury H, Lai KM, Peschard P, Dankort D, Naujokas MA, Holash J, Yancopoulos GD, Muller WJ, Pawson T, Park M: The Shc adaptor protein is critical for VEGF induction by Met/HGF and ErbB2 receptors and for early onset of tumor angiogenesis. Proc Natl Acad Sci U S A 2004, 101:2345–2350
28. Matsumoto K, Nakamura T: Hepatocyte growth factor and the Met system as a mediator of tumor-stromal interactions. Int J Cancer 2006, 119:477–483
29. Chen JT, Huang CY, Chiang YY, Chen WH, Chiou SH, Chen CY, Chow KC: HGF increases cisplatin resistance via down-regulation of AIF in lung cancer cells. Am J Respir Cell Mol Biol 2008, 38:559–565
30. Hayashida M, Kawano H, Nakano T, Shiraki K, Suzuki A. Hepatocyte growth factor promotes cell survival from fas-mediated cell death in hepatocellular carcinoma cells via Akt activation and Fas-death-inducing signaling complex suppression. Hepatology 2000, 32:796–802
31. Zeng Q, McCauley LK, Wang CY: Hepatocyte growth factor inhibits anoikis by induction of activator protein 1-dependent cyclooxygenase-2: implication in head and neck squamous cell carcinoma progression. J Biol Chem 2002, 277:50137–50142
32. Shojaei F, Lee JH, Simmons BH, Wong A, Esparza CO, Plumlee PA, Feng J, Stewart AE, Hu-Lowe DD, Christensen JG: HGF/c-Met acts as an alternative angiogenic pathway in sunitinib-resistant tumors. Cancer Res 2010, 70:10090–10100
33. Casanovas O, Hicklin DJ, Bergers G, Hanahan D: Drug resistance by evasion of antiangiogenic targeting of VEGF signaling in late-stage pancreatic islet tumors. Cancer Cell 2005, 8:299–309
34. Höckel M, Vaupel P: Tumor hypoxia: definitions and current clinical, biologic, and molecular aspects. J Natl Cancer Inst 2001, 93:266–276
35. Pennacchietti S, Michieli P, Galluzzo M, Mazzone M, Giordano S, Comoglio PM: Hypoxia promotes invasive growth by transcriptional activation of the met protooncogene. Cancer Cell 2003, 3:347–361
36. Jain RK: Molecular regulation of vessel maturation. Nat Med 2003, 9:685–693
37. Zhang S, Zhau HE, Osunkoya AO, Iqbal S, Yang X, Fan S, Chen Z, Wang R, Marshall FF, Chung LW, Wu D: Vascular endothelial growth factor regulates myeloid cell leukemia-1 expression through neuropilin-1-dependent activation of c-MET signaling in human prostate cancer cells. Mol Cancer 2010, 9:9
38. Mitsudomi T, Yatabe Y: Mutations of the epidermal growth factor receptor gene and related genes as determinants of epidermal growth factor receptor tyrosine kinase inhibitors sensitivity in lung cancer. Cancer Sci 2007, 98:1817–1824
39. Kasahara K, Arao T, Sakai K, Matsumoto K, Sakai A, Kimura H, Sone T, Horiike A, Nishio M, Ohira T, Ikeda N, Yamanaka T, Saijo N, Nishio K: Impact of serum hepatocyte growth factor on treatment response to epidermal growth factor receptor tyrosine kinase inhibitors in patients with non-small cell lung adenocarcinoma. Clin Cancer Res 2010, 16:4616–4624
40. Tanaka H, Kimura T, Kudoh S, Mitsuoka S, Watanabe T, Suzumura T, Tachibana K, Noguchi M, Yano S, Hirata K: Reaction of plasma hepatocyte growth factor levels in non-small cell lung cancer patients treated with EGFR-TKIs. Int J Cancer 2011, 129:1410–1416
41. Han JY, Kim JY, Lee SH, Yoo NJ, Choi BG: Association between plasma hepatocyte growth factor and gefitinib resistance in patients with advanced non-small cell lung cancer. Lung Cancer 2011, 74:293–299

Published OnlineFirst May 2, 2012; DOI: 10.1158/1078-0432.CCR-11-2972

Cancer Therapy: Preclinical

Clinical Cancer Research

Paracrine Receptor Activation by Microenvironment Triggers Bypass Survival Signals and ALK Inhibitor Resistance in EML4-ALK Lung Cancer Cells

Tadaaki Yamada[1], Shinji Takeuchi[1], Junya Nakade[1], Kenji Kita[1], Takayuki Nakagawa[1,2], Shigeki Nanjo[1], Takahiro Nakamura[3], Kunio Matsumoto[3], Manabu Soda[4], Hiroyuki Mano[4], Toshimitsu Uenaka[2], and Seiji Yano[1]

Abstract

Purpose: Cancer cell microenvironments, including host cells, can critically affect cancer cell behaviors, including drug sensitivity. Although crizotinib, a dual tyrosine kinase inhibitor (TKI) of ALK and Met, shows dramatic effect against *EML4-ALK* lung cancer cells, these cells can acquire resistance to crizotinib by several mechanisms, including ALK amplification and gatekeeper mutation. We determined whether microenvironmental factors trigger ALK inhibitor resistance in *EML4-ALK* lung cancer cells.

Experimental Design: We tested the effects of ligands produced by endothelial cells and fibroblasts, and the cells themselves, on the susceptibility of *EML4-ALK* lung cancer cell lines to crizotinib and TAE684, a selective ALK inhibitor active against cells with *ALK* amplification and gatekeeper mutations, both *in vitro* and *in vivo*.

Results: *EML4-ALK* lung cancer cells were highly sensitive to ALK inhibitors. EGF receptor (EGFR) ligands, such as EGF, TGF-α, and HB-EGF, activated EGFR and triggered resistance to crizotinib and TAE684 by transducing bypass survival signaling through Erk1/2 and Akt. Hepatocyte growth factor (HGF) activated Met/Gab1 and triggered resistance to TAE684, but not crizotinib, which inhibits Met. Endothelial cells and fibroblasts, which produce the EGFR ligands and HGF, respectively, decreased the sensitivity of *EML4-ALK* lung cancer cells to crizotinib and TAE684, respectively. EGFR-TKIs resensitized these cells to crizotinib and Met-TKI to TAE684 even in the presence of EGFR ligands and HGF, respectively.

Conclusions: Paracrine receptor activation by ligands from the microenvironment may trigger resistance to ALK inhibitors in *EML4-ALK* lung cancer cells, suggesting that receptor ligands from microenvironment may be additional targets during treatment with ALK inhibitors. *Clin Cancer Res; 18(13); 3592–602. ©2012 AACR.*

Introduction

ALK fusion with EML4 in non–small cell lung cancer (NSCLC) was first detected in 2007 (1), with 3% to 7% of unselected NSCLCs having this fusion gene (1–4). EML4-ALK lung cancer is more frequently observed in patients with adenocarcinoma than with other histologies, in young adults than in older patients, and in never-smokers or light smokers (<15 pack-years) than in heavier smokers (2, 3). ALK kinase inhibitors show dramatic effects against lung cancers with *EMK4-ALK in vitro* and *in vivo* (3, 4). In a phase I–II trial with crizotinib, a dual tyrosine kinase inhibitor (TKI) of ALK and Met, the overall response rate was 47 of 82 (57%) patients with *EML4-ALK*–positive tumors (5). However, almost all patients who show a marked response to ALK-TKIs acquire resistance to these agents after varying periods of time (6, 7). Secondary mutations, including the gatekeeper L1196M mutation and others (F1174L, C1156Y, G1202R, S1206Y, 1151-T-ins, and G1269A), *ALK* amplification, *KIT* amplification, and autophosphorylation of EGF receptor (EGFR), were shown to be responsible for acquired resistance to crizotinib in ALK-translocated cancers (6–10).

Selective ALK inhibitors, including TAE684 and CH5424802, have been reported active against *EML4-ALK* lung cancer cells with *ALK* amplification and secondary mutations. These cells, however, may develop resistance to this class of inhibitor, due to several mechanisms, including novel *ALK* mutations (L1152R, L1198P, and D1203N), coactivation of EGFR and ErbB2, and EGFR phosphorylation (3, 11, 12).

Authors' Affiliations: [1]Division of Medical Oncology, Cancer Research Institute, Kanazawa University, Kanazawa, Ishikawa; [2]Tsukuba Research Laboratories, Eisai co., ltd., Ibaraki; [3]Division of Tumor Dynamics and Regulation, Cancer Research Institute, Kanazawa University, Kanazawa, Ishikawa; and [4]Division of Functional Genomics, Jichi Medical University, Shimotsuke, Tochigi, Japan

Note: Supplementary data for this article are available at Clinical Cancer Research Online (http://clincancerres.aacrjournals.org/).

Corresponding Author: Seiji Yano, Division of Medical Oncology, Cancer Research Institute, Kanazawa University 13-1, Takara-machi, Kanazawa, Ishikawa 920-0934, Japan. Phone: 81-76-265-2794; Fax: 81-76-234-4524; E-mail: syano@staff.kanazawa-u.ac.jp

doi: 10.1158/1078-0432.CCR-11-2972

Published OnlineFirst May 2, 2012; DOI: 10.1158/1078-0432.CCR-11-2972

Translational Relevance

Although crizotinib, a dual inhibitor of ALK and Met, shows dramatic effects against *EML4-ALK* lung cancer cells, these cells can acquire resistance by several mechanisms, including ALK amplification and gatekeeper mutation. Selective ALK inhibitors may overcome crizotinib resistance due to these mechanisms, but these cells may become resistant to these inhibitors.

We show here that EGF receptor ligands produced by endothelial cells can cause *EML4-ALK* lung cancer cells to become resistant to crizotinib and selective ALK inhibitors by triggering bypass survival signals. By contrast, hepatocyte growth factor produced by fibroblasts can induce resistance to selective ALK inhibitors, but not crizotinib. Because endothelial cells and fibroblasts are components of the microenvironment, our findings raise clinical questions about the class of ALK inhibitors more beneficial for *EML4-ALK* lung cancer patients. Moreover, our results provide a rationale for targeting receptor ligands in the microenvironment for more successful treatment with ALK inhibitors.

Most human cancers are composed of cancer cells that coexist with a variety of extracellular matrix components and cell types, including fibroblasts, endothelial cells, and immune cells, which collectively form the tumor microenvironment (13). This microenvironment can influence the growth, survival, invasiveness, metastatic ability, and drug sensitivity of cancer cells within these tumors (14). Paracrine signaling between cancer cells and host cells in the microenvironment, mediated by cytokines, chemokines, growth factors, and other signaling molecules, plays a critical role in tumor growth (15). As receptors for these factors, the EGFR family of receptors and Met are of particular interest in lung cancer (16). The EGFR family consists of at least 4 receptor tyrosine kinases, including EGFR (ErbB1), Her2/neu (ErbB2), HER3 (ErbB3), and HER4 (ErbB4). To date, 7 ligands for EGFR have been identified: EGF, TGF-α; heparin-binding EGF-like growth factor (HB-EGF); amphiregulin; betacellurin; epiregulin; and epigen (17). By contrast, Met is the only specific receptor for hepatocyte growth factor (HGF) and HGF binds only to Met (18). Many lung cancer cells express EGFR and Met, with these cells and others in their microenvironment expressing their ligands (19, 20), suggesting that these receptors and ligands modulate the sensitivity of cancer cells to molecular targeted drugs in their microenvironment. We previously showed that fibroblast-derived HGF induces EGFR-TKI resistance in *EGFR*-mutant lung cancer cells by activating Met and downstream pathways (21, 22). However, the role of the microenvironment in the sensitivity of EML4-ALK lung cancer cells to ALK-TKIs has not been determined. We therefore examined whether factors in the microenvironment of *EML4-ALK* lung cancer cells trigger their resistance to crizotinib and TAE684, a selective ALK inhibitor, as well as clarifying their underlying mechanisms of action.

Materials and Methods

Cell culture

The H2228 human lung adenocarcinoma cell line, with the EML4-ALK fusion protein variant3 (E6;A20), the umbilical vein endothelial cell line human umbilical vein endothelial cells (HUVEC) and the human bronchial epithelial cell line BEAS-2B, transformed with SV40 virus, were purchased from the American Type Culture Collection. The H3122 human lung adenocarcinoma cell line, with the EML4-ALK fusion protein variant1 (E13;A20), was kindly provided by Dr. Jeffrey A. Engelman of the Massachusetts General Hospital Cancer Center, Boston, MA (3). The MANA2 mouse lung adenocarcinoma cell line was established in Jichi Medical University from a tumor nodule developed in a transgenic mouse expressing *EML4-ALK* variant 1 (E13;A20) (23). The MRC-5 and IMR-90 lung embryonic fibroblast cell lines were obtained from RIKEN Cell Bank. The human dermal microvessel endothelial cell line HMVEC was purchased from Kurabo. The monocytic leukemia cell line U937 was purchased from Health Science Research Resources Bank. H2228 cells were cultured in RPMI-1640 medium, MANA2 cells were cultured in DMEM/F12+GlutaMAX-1, and MRC-5 (P 25–30) cells were cultured in Dulbecco's modified Eagle's medium (DMEM) medium, supplemented with 5% fetal bovine serum, penicillin (100 U/mL), and streptomycin (50 μg/mL), in a humidified CO_2 incubator at 37°C. HMVECs and HUVECs were maintained in HuMedia-MvG with growth supplements (Kurabo) and used for *in vitro* assays at passages 2 to 5 and 2 to 4, respectively. BEAS-2B cells were maintained in LHC9/RPMI-1640 medium, as described (24), and used for *in vitro* assays at passages 42 to 46. Macrophage differentiation of U937 cells was induced by incubation in RPMI-1640 medium containing 10 ng/mL phorbol 12-myristate 13-acetate (Sigma Chemical Co.; ref. 25) for 5 days, with floating cells removed by rinsing with PBS, as described (26). Differentiated U937 cells (PMA-U937 cells) attached to the dishes were used for *in vitro* assays at passages 6 to 8. All cells were passaged for less than 3 months before renewal from frozen, early-passage stocks obtained from the indicated sources. Cells were regularly screened for *Mycoplasma* using a MycoAlert *Mycoplasma* Detection Kit (Lonza).

Reagents

TAE684, crizotinib, and WZ4002 were purchased from Seleck Chemicals. Erlotinib hydrochloride was obtained from Chugai Pharmaceutical Co., Ltd. The anti-human EGFR antibody cetuximab was obtained from Merck Serono. E7050 was synthesized by Eizai Co., Ltd. (27). Goat anti-human HGF antibody, control goat IgG, recombinant EGF, TGF-α, HB-EGF, IGF-1, and PDGF-AA were purchased from R&D Systems. Recombinant HGF was prepared as described (28).

Published OnlineFirst May 2, 2012; DOI: 10.1158/1078-0432.CCR-11-2972

Cell growth assay

Cell proliferation was measured using the MTTdye reduction method (17). Tumor cells at 80% confluence were harvested, seeded at 2×10^3 cells per well in 96-well plates, and incubated in appropriate medium for 24 hours. Several concentrations of TAE684, crizotinib, erlotinib, WZ4002, E7050, cetuximab, anti-HGF antibody, and/or EGF, TGF-α, HB-EGF, IGF-1, PDGF-AA, and HGF were added to each well, and incubation was continued for a further 72 hours. To each well was added 50 μL MTT (2 mg/mL; Sigma), followed by incubation for 2 hours at 37°C. The media were removed and the dark blue crystals in each well were dissolved in 100 μL of dimethyl sulfoxide (DMSO). Absorbance was measured with an MTP-120 Microplate reader (Corona Electric) at test and reference wavelengths of 550 and 630 nm, respectively. The percentage growth was calculated relative to untreated controls. Each assay was carried out at least in triplicate, with results based on 3 independent experiments.

Apoptosis assay

H2228 and H3122 cells (3×10^3 cells) were seeded in 96-well, white-walled plates and incubated overnight. The cells were treated with crizotinib (1 μmol/L) or vehicle (DMSO) for 48 hours. Cellular apoptosis was determined by measuring caspase-3/7 activity using a luminometric Caspase-Glo 3/7 assay (Promega) according to the manufacturer's protocol, with luminescence intensity measured using a Fluoroskan Ascent FL plate reader (Thermo Scientific). Cellular apoptosis was expressed relative to DMSO-treated control cells.

RNA interference

Duplexed Stealth RNAi (Invitrogen) against *EGFR*, *Met*, *ErbB3*, *Gab1*, *ALK*, and Stealth RNAi-negative control low GC Duplex #3 (Invitrogen) were used for RNA interference (RNAi) assays. Briefly, aliquots of 1×10^5 cells in 2 mL of antibiotic-free medium were plated into each well of a 6-well plate and incubated at 37°C for 24 hours. The cells were transfected with siRNA (250 pmol) or scrambled RNA using Lipofectamine 2000 (5 μL) in accordance with the manufacturer's instructions (Invitrogen). After 24 hours, the cells were washed twice with PBS and incubated with or without crizotinib (100 nmol/L), TAE684 (100 nmol/L), recombinant human EGF (100 ng/mL), TGF-α (100 ng/mL), HB-EGF (10 ng/mL), or HGF (50 ng/mL) for an additional 48 hours in antibiotic-containing medium. These tumor cells were then used for cell proliferation assays, with *EGFR*, *Met*, *ErbB3*, *Gab1*, and *ALK* knockdowns (#1, #2) confirmed by Western blotting.

The siRNA target sequences were as follows: *EGFR*, 5′-CGGAATAGGTATTGGTGAATTTAAA-3′ and 5′-UUUAAAUUCACCAAUACCUAUUCCG-3′, *Met*, 5′-UCCAGAAGAUCAGUUUCCUAAUUCA-3′ and 5′-UGAAUUAGGAAACUGAUCUUCUGGA-3′, *ErbB3*, 5′-GGCCAUGAAUGAAUUCUCUACUCUA-3′ and 5′-UAGAGUAGAGAAUUCAUUCAUGGCC-3′, *Gab1*, 5′-UAGAGUAGCAGAGGAUGAAUCUGCC-3′ and 5′-GGCAGAUUCAUCCUCUGCUACUCUA-3′, *ALK #1*, 5′-UCAUUAUCCGGUAUACAGGCCCAGG-3′ and 5′-CCUGGGCCUGUAUACCGGAUAAUGA-3′, and ALK #2, 5′-AAAGCUGCACUCCAGACCAUAUCGG-3′ and 5′-CCGAUAUGGUCUGGAGUGCAGCUUU-3′. Each assay was carried out at least in triplicate, with 3 independent experiments conducted.

Western blotting

SDS polyacrylamide gels (Bio-Rad) were loaded with 40 μg total protein per lane; following electrophoresis, the proteins were transferred onto polyvinylidene difluoride membranes (Bio-Rad), which were incubated with Blocking One (Nacalai Tesque) for 1 hour at room temperature, followed by overnight incubation at 4°C with anti-ALK (C26G7), anti–phospho-ALK (Tyr1604), anti–phospho-EGFR (Tyr1068), anti-STAT-3(79D7), anti–phospho-STAT-3 (Y705), anti-Akt, anti–phospho-Akt (Ser473), anti-ErbB4 (111B2), anti–phospho-ErbB4 (Tyr1284), anti-Met (25H2), anti–phospho-Met (Y1234/Y1235) (3D7), anti-Gab1 (#3232), anti-phospho-Gab1 (Tyr627) (C32H2), anti-ErbB3 (1B2), anti–phospho-ErbB3 (Tyr1289) (21D3), or anti-β-actin (13E5) antibodies (1:1,000 dilution each; Cell Signaling Technology), or with anti-human EGFR (1 μg/mL), anti-human/mouse/rat extracellular signal-regulated kinase (Erk)1/Erk2 (0.2 μg/mL), or anti-phospho-Erk1/Erk2 (T202/Y204) (0.1 μg/mL) antibodies (R&D Systems). After washing 3 times, the membranes were incubated for 1 hour at room temperature with secondary Ab (horseradish peroxidase–conjugated species-specific Ab). Immunoreactive bands were visualized with SuperSignal West Dura Extended Duration Substrate Enhanced Chemiluminescent Substrate (Pierce). Each experiment was carried out at least 3 times independently.

HGF, EGF, TGF-α, and HB-EGF production in cell culture supernatant

Cells (2×10^5) were cultured in 2 mL of RPMI-1640 or DMEM with 5% FBS for 24 hours. The cells were washed with PBS and incubated for 48 hours in RPMI-1640 or DMEM with 5% FBS. The culture medium was harvested and centrifuged, and the supernatant was stored at −70°C until analysis. HGF (Immunis HGF EIA; B-Bridge International), EGF, TGF-α, and HB-EGF (Quantikine ELISA kits; R&D Systems) were assayed by ELISA, in accordance with the manufacturer's procedures. All samples were run in triplicate. Color intensity was measured at 450 nm with a spectrophotometric plate reader. Growth factor concentrations were determined by comparison with standard curves. The detection limits for HGF, EGF, TGF-α, and HB-EGF were 0.1 ng/mL, 3.9 pg/mL, 15.6 pg/mL, and 31.2 pg/mL, respectively.

Coculture of lung cancer cells with fibroblasts or endothelial cells

Cells were cocultured in Transwell Collagen-Coated chambers separated by an 8-μm (BD Biosciences, Erembodegem) or 3-μm (Corning Costar) pore size filter. Tumor cells (8×10^3 cells/800 μL) with or without TAE684

Published OnlineFirst May 2, 2012; DOI: 10.1158/1078-0432.CCR-11-2972

(100 nmol/L) or crizotinib (100 nmol/L) in the lower chamber were cocultured with MRC-5 (1×10^4 cells/300 μL) or HMVEC (1×10^4 cells/300 μL) cells, with or without 2 hours of pretreatment with anti-human HGF antibody (2 μg/mL) or cetuximab (2 μg/mL) in the upper chamber for 72 hours. The upper chamber was then removed, 200 μL of MTT solution (2 mg/mL; Sigma) was added to each well and the cells were incubated for 2 hours at 37°C. The media were removed and the dark blue crystals in each well were dissolved in 400 μL of DMSO. Absorbance was measured with an MTP-120 Microplate reader (Corona Electric) at test and reference wavelengths of 550 and 630 nm, respectively. The percentage growth was measured relative to untreated controls. All samples were assayed at least in triplicate, with each experiment conducted 3 times independently.

Xenograft studies in SCID mice

Suspensions of H2228 cells (5×10^6), with or without MRC-5 cells (5×10^6), were injected subcutaneously into the backs of 5-week-old male severe combined immunodeficient (SCID) mice (Japan Clea). After 4 days (tumors diameter >4 mm), mice were randomly allocated into groups of 6 animals to receive TAE684 (1.25 mg/kg/d) or vehicle by oral gavage. Tumor size was measured with digital calipers, and tumor volume was calculated as 0.5 × length × (width)^2. All animal experiments complied with the Guidelines for the Institute for Experimental Animals, Kanazawa University Advanced Science Research Center (approval no. AP-081088).

HGF production in tumor tissues

Tumors obtained from SCID mice after 4 and 8 days were lysed in mammalian tissue lysis buffer containing a phosphatase and proteinase inhibitor cocktail (Sigma). HGF was quantitated by ELISA (Immunis HGF EIA; Institute of Immunology), with a detection limit of 0.1 ng/mL. All samples were assayed in triplicate.

Statistical analysis

Differences were analyzed by one-way ANOVA. All statistical analyses were carried out using GraphPad Prism Ver. 4.01 (GraphPad Software, Inc.). $P < 0.05$ was considered significant.

Results

HGF and/or EGFR ligands reduced the sensitivity of EML4-ALK lung cancer cells to ALK inhibitor *in vitro*

We first examined the sensitivity of human H2228, human H3122, and mouse MANA2 lung cancer cell lines, all containing EML4-ALK translocations, to the ALK inhibitors crizotinib and TAE684, and to various EGFR-TKIs. Human H2228 cells with *EML4-ALK* variant 3 (E6;A20) and H3122 cells with *EML4-ALK* variant 1 (E13;A20) were insensitive to the EGFR-TKIs erlotinib (a reversible EGFR-TKI) and WZ4002 (selective for mutant EGFR), but sensitive to the ALK-TKIs crizotinib and TAE684 (Fig. 1). MANA2 cells, established from lung tumors of an *EML4-ALK* variant 1 (E13;A20) transgenic mouse, were also sensitive to crizotinib and TAE684, although their viability was slightly inhibited by high concentrations (1 μmol/L) of EGFR-TKIs.

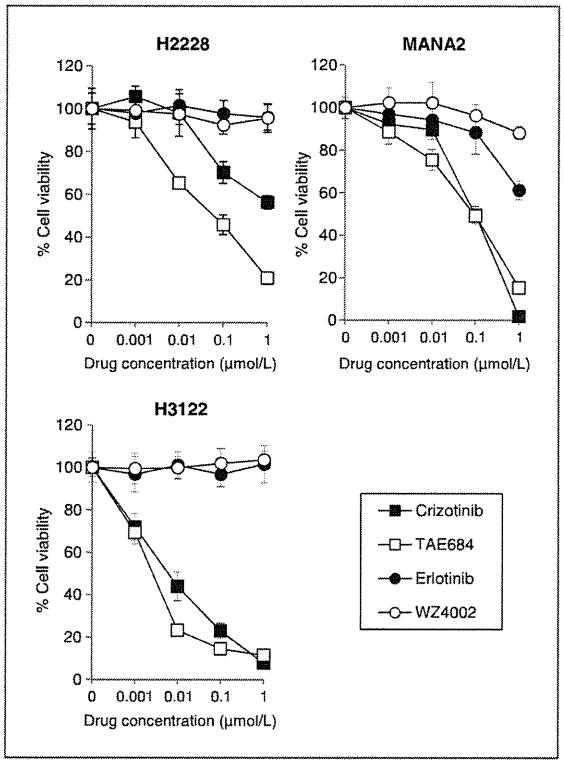

Figure 1. EML4-ALK lung cancer cells are highly sensitive to the ALK inhibitors, crizotinib, and TAE684. The sensitivity of EML4-ALK lung cancer cells, human H2228, human H3122, and mouse MANA2, to the ALK inhibitors, crizotinib, and TAE684 were determined by analyzing the effects of the EGFR-TKIs, erlotinib (reversible EGFR-TKI), and WZ4002 (mutant EGFR selective TKI). Tumor cell growth after 72 hours was measured by the MTT assay. Each sample was assayed in triplicate, with each experiment repeated at least 3 times independently.

Because several growth factors have been associated with poor patient prognosis and/or drug resistance in lung cancer, we explored the effect of EGFR ligands (EGF, TGF-α, and HB-EGF), IGF-1, PDGF-AA, and HGF on the sensitivity of *EML4-ALK* lung cancer cells to ALK inhibitors. In the absence of ALK inhibitors, these growth factors slightly increased the viability of H2228, H3122, and MANA2 cells. In H2228 cells, all 3 EGFR ligands reduced sensitivity to crizotinib in a dose-dependent manner, but IGF-1, PDGF-AA, and HGF failed to do so (Fig. 2, Supplementary Fig. S1). Interestingly, HGF, as well as the EGFR ligands, reduced sensitivity to TAE684, but IGF-1 and PDGF-AA failed to do so. Similar results were observed in H3122 and MANA2 cells. To further confirm the effect of these growth factors on specific ALK inhibition, we knocked down ALK using 2 different specific siRNAs in H2228 cells. Whereas H2228 cells were highly sensitive to *ALK*-specific siRNAs, EGFR ligands and HGF restored cell viability inhibited by ALK knockdown (Supplementary Fig. S2). When we

Published OnlineFirst May 2, 2012; DOI: 10.1158/1078-0432.CCR-11-2972

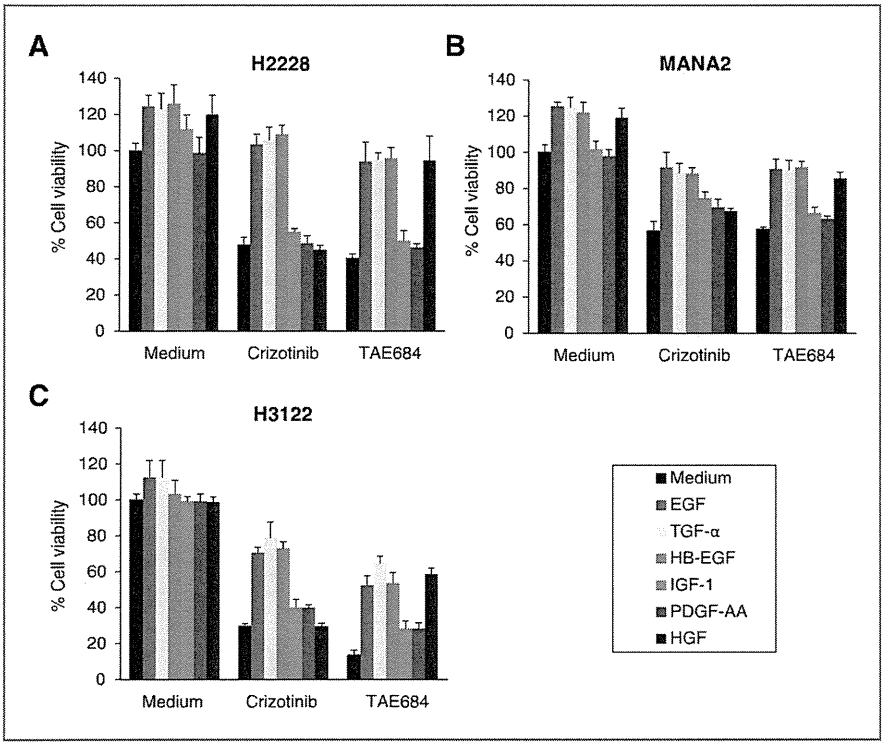

Figure 2. HGF and/or EGFR ligands (EGF, TGF-α, and HB-EGF) reduce the sensitivity of EML4-ALK lung cancer cells to ALK inhibitors *in vitro*. H2228, H3122, and MANA2 cells were incubated with or without crizotinib (100 nmol/L), TAE684 (100 nmol/L), and/or EGF, TGF-α, IGF-I, or PDGF-AA (100 ng/mL); HB-EGF (10 ng/mL), or HGF (50 ng/mL), with cell growth determined after 72 hours. The percentage growth is shown relative to untreated controls. Each sample was assayed in triplicate, with each experiment repeated at least 3 times independently.

assessed the ability of crizotinib to induce apoptosis in H2228 and H3122 cells, we found that crizotinib induced apoptosis in H3122, but not H2228, cells (Supplementary Fig. S3).

HGF and EGFR ligands trigger ALK inhibitor resistance via Met and EGFR, respectively

To assess the mechanism by which these growth factors reduced cell sensitivity to ALK inhibitors, we analyzed the phosphorylation status of ALK, receptors, and their downstream molecules in H2228, H3122, and MANA2 cells by Western blotting. Crizotinib inhibited ALK phosphorylation, thereby suppressing the phosphorylation of Akt, Erk1/2 and STAT-3, as described (ref. 11; Fig. 3A, Supplementary Fig. S4). The EGFR ligands, EGF, TGF-α, and HB-EGF stimulated EGFR phosphorylation. Crizotinib inhibited ALK and STAT-3 phosphorylation even in the presence of EGFR ligands, but failed to inhibit phosphorylation of EGFR and downstream Akt, and Erk1/2. Phosphorylation of ErbB4, a potential receptor for HB-EGF, was not affected by crizotinib or EGFR ligands. To further confirm the involvement of EGFR in crizotinib resistance induced by EGFR ligands, we knocked down EGFR by specific siRNAs in H2228 and H3122 cells (Fig. 3B). Although crizotinib markedly inhibited cell viability and all 3 EGFR ligands induced resistance in cells treated with scrambled siRNA, resistance to crizotinib was not induced by EGF, TGF-α, or HB-EGF in EGFR siRNA-treated cells, indicating that EGFR ligand-triggered crizotinib resistance is mediated by EGFR.

In parallel experiments, TAE684 inhibited ALK phosphorylation, thereby suppressing the phosphorylation of Akt, Erk1/2, and STAT-3 (Fig. 3C). HGF stimulated the phosphorylation of Met and its adaptor protein, Gab1, as described (29). TAE684 inhibited ALK and STAT-3 phosphorylation even in the presence of HGF, but failed to inhibit phosphorylation of Met and downstream Akt and Erk1/2. Phosphorylation of ErbB3, an adaptor of amplified, but not HGF-stimulated Met (30), was not affected by TAE684 or HGF. To further confirm the involvement of Met and Gab1 in HGF-induced TAE684 resistance, we knocked down Met, ErbB3, or Gab1 by specific siRNAs in H2228 and H3122 cells (Fig. 3D). TAE684 markedly inhibited the viability and HGF induced resistance in cells treated with scrambled siRNA. Importantly, treatment of cells with Met or Gab1, but not ErbB3, siRNA, induced TAE684 resistance, indicating the involvement of Met/Gab1 in HGF-induced resistance to TAE684.

Cross-talk of endothelial cells and fibroblasts reduces the sensitivity of EML4-ALK lung cancer cells to ALK inhibitors

To determine which types of host cells could produce EGFR ligands and HGF, we investigated production of these growth factors by various types of host stromal cells, comparing lung epithelial cells and cancer cells. The endothelial cell lines HMVEC produced discernible levels of EGFR ligands, including EGF, TGF-α, and HB-EGF, whereas fibroblasts produced a high level of HGF (Fig. 4A). EML4-ALK lung cancer cells (H2228, H3122, and